(NASA-CR-146433) THECRETICAL AND EXPERIMENTAL STUDIES CF ATMOSPHERIC STRUCTURE AND DYNAMICS, USING HIGH ALTITUDE CHEMICAL RELEASE, RADIO METEOR, AND METEOROLOGICAL ROCKET NETWORK AND (Georgia G3/46

N76-19638
HC $4.50
Unclas
20598

GEORGIA INSTITUTE OF TECHNOLOGY

SEMI-ANNUAL STATUS REPORT NO. 27

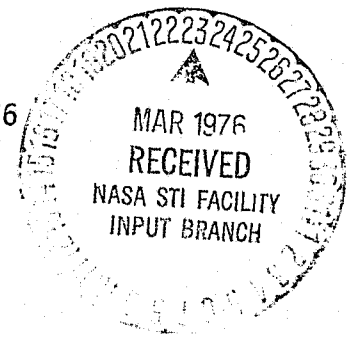

REPORTING PERIOD: 1 September 1975 to 29 February 1976

Grant No. NGL 11-002-004
Georgia Tech Project No. E-16-605

GRANT PBJECTIVE: Theoretical and Experimental Studies of Atmospheric Structure and Dynamics, Using High Altitude Chemical Release, Radio Meteor, and Meteorological Rocket Network and Other Data

GRANT SPONSOR: National Aeronautics and Space Administration
Washington, D. C.

PRINCIPAL INVESTIGATOR: Howard D. Edwards

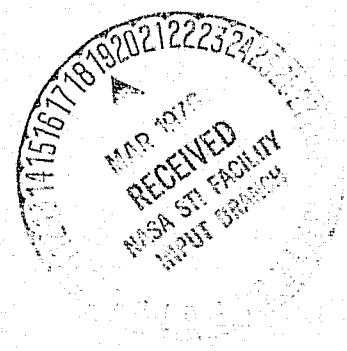

RESEARCH ACTIVITIES

Analysis of the data collected by the Georgia Tech Radio Meteor Wind Facility during the fall and winter of 1975 has revealed a difference in the prevailing zonal component from that observed in 1974. The easterlies observed in '74 have been replaced by westerlies in 1975. This is of particular interest in that there was a major stratwarm in the '74 winter, but only a minor event in '75. It appears that the relationship between lower thermospheric circulation at mid latitudes and polar stratospheric dynamics, as detailed in the last semiannual report, is real and warrants further investigation.

A paper "Turbulence in the Lower Thermosphere" (copy attached) has been written for inclusion in the monograph on the upper atmosphere to be published by the Geophysics Research Board of the National Academy of Sciences.

A diffusion simulation program is being developed and studied which uses the Global Reference Atmosphere program to follow the trajectory of a simulated pollutant cloud and simulates its turbulent diffusive spread as it moves through the atmosphere. Applications envisioned are study of far wake diffusion of SST's and the Space Shuttle. The diffusive spread of the cloud is modeled by a time step evaluation of the assumed Gaussian standard deviations (σ_x, σ_y, and σ_z) by the relations:

$$\sigma_x^2(t + \Delta t) = \sigma_x^2(t) + \sigma_u^2(1 - \bar{\rho}_u)\,\Delta t^2 \qquad (1)$$

$$\sigma_y^2(t + \Delta t) = \sigma_y^2(t) + \sigma_v^2(1 - \bar{\rho}_v)\,\Delta t^2 \qquad (2)$$

$$\sigma_z^2(t + \Delta t) = \sigma_z^2(t) + \sigma_w^2(1 - \bar{\rho}_w)\,\Delta t^2 \qquad (3)$$

where σ_u, σ_v, and σ_w are the magnitudes of the turbulence (or random small scale gravity wave) fields, and $\bar{\rho}_u$, $\bar{\rho}_v$, and $\bar{\rho}_w$ are the correlation functions of the turbulent velocity field averaged over the spatial dimensions of the Gaussian cloud (with the Gaussian cloud distribution as a spatial weighting function). Different values for σ_u, σ_v, and σ_w can be input, as well as different length scales for the components of the correlation ρ_u, ρ_v, and ρ_w. Therefore, anisotropic diffusion (larger in the horizontal than vertical) can be simulated with the model.

Diffusive processes simulated by equations (1 - 3) have been found to in-

crease rapidly after initial release of the simulated cloud, but with eventual approach to $\sigma_x^2 \propto 2K_x t$ and $\sigma_z^2 \propto 2K_z t$ eddy diffusion at large cloud sizes (σ's greater than the turbulence length scales).

PUBLICATIONS

"A Global Reference Atmospheric Model for Surface to Orbital Altitudes", Journal of Applied Meteorology, 15, 3-9, January 1976, C. G. Justus, R. G. Roper, A. Woodrum, and O. E. Smith (reprint attached).

"Turbulence in the Lower Thermosphere", presented at the Fall AGU meeting, December 8-12, 1975 San Francisco, to be published in a monograph by the Geophysics Research Board of the National Academy of Science, R. G. Roper.

PLANS FOR THE NEXT PERIOD

Analysis of Georgia Tech radio meteor wind data gathered over the period of the winter anomaly rocket program carried out in January 1976 at Wallops Island will be undertaken.

Organization of publication of a set of papers written by participants in the URSI/IAGA Cooperative Tidal Experiments is proceeding.

Development and study will continue on the diffusion model based on the Global Reference Atmosphere. With the height and latitude dependent parameters of small scale velocity perturbation magnitudes σ_u and length scale L built into the model, the eddy diffusion coefficients K_x and K_z for horizontal and vertical diffusion can be evaluated and related to the input σ_u and L values. The K_x and K_z values thus determined should prove useful for global circulation modelers who need one or two dimensional variation profiles of K_z and/or K_x.

Respectfully submitted:

Howard D Edwards

Howard D. Edwards
Principal Investigator

Reprinted from JOURNAL OF APPLIED METEOROLOGY, Vol. 15, No. 1, January 1976
American Meteorological Society
Printed in U. S. A.

A Global Reference Atmospheric Model for Surface to Orbital Altitudes

C. G. JUSTUS AND R. G. ROPER

School of Aerospace Engineering, Georgia Institute of Technology, Atlanta 30332

ARTHUR WOODRUM

School of Physics, Georgia Southern College, Statesboro 30458

O. E. SMITH

Aerospace Environment Division, NASA, Marshall Space Flight Center, Alabama 35812

(Manuscript received 9 June 1975, in revised form 26 September 1975)

ABSTRACT

An empirical atmospheric model has been developed which generates values for pressure, density, temperature and winds from surface levels to orbital altitudes. The output parameters consist of components for: 1) latitude, longitude, and altitude dependent monthly means; 2) quasibiennial oscillations; and 3) random perturbations to partially simulate the variability due to synoptic, diurnal, planetary wave and gravity wave variations. The monthly mean models consist of: (i) NASA's four dimensional worldwide model, developed by Environmental Research and Technology, for height, latitude, and longitude dependent monthly means from the surface to 25 km; and (ii) a newly developed latitude-longitude dependent model which is an extension of the Groves latitude dependent model for the region between 25 and 90 km. The Jacchia 1970 model is used above 90 km and is faired with the modified Groves values between 90 and 115 km. Quasi-biennial and random variation perturbations are computed from parameters determined from various empirical studies, and are added to the monthly mean values. This model has been developed as a computer program which can be used to generate altitude profiles of atmospheric variables for any month at any desired location, or to evaluate atmospheric parameters along any simulated trajectory through the atmosphere. Various applications of the model are discussed, and results are presented which show that good simulation of the thermodynamic and circulation characteristics of the atmosphere can be achieved with the model.

1. Introduction

In response to needs for an engineering oriented global reference atmospheric model, a computer model has been developed at Georgia Tech which gives pressure, temperature, density and wind variables and their structure as a function of the three spatial coordinates—latitude, longitude, altitude—and time (monthly, plus statistically consistent perturbations about the monthly mean). The altitude range is from sea level to about 700 km.

The new computer program combines the previously developed Jacchia (1970) model for above 115 km, the four-dimensional (4-D) model of Spiegler and Fowler (1972) for below 25 km, and a newly developed latitude-longitude dependent model, which is an extension of the Groves (1971) model for the region between 30 and 90 km. Between 90 and 115 km a smooth transition between the modified Groves values and the Jacchia values is accomplished by a fairing technique (a combination of Groves and Jacchia values which insures smooth transition from Groves below 90 km to Jacchia above 115 km). Between 25 and 30 km an interpolation scheme is used between the 4-D results and the modified Groves values. Interpolation is also used to fill in between the discrete height, latitude and longitude intervals of data values on the input data tapes. On the 0 to 25 km tapes the resolution is 1 km in height and roughly 5°×5° in latitude and longitude. For the modified Groves section the resolution is 5 km in height, 10° latitude for zonal mean, and 20° latitude by 30° longitude for the modification to the zonal means.

In addition to monthly mean values of pressure, density, temperature and winds, two types of perturbations are evaluated: quasi-biennial and random. The quasi-biennial oscillations in pressure, density, temperature and winds, empirically determined to be represented by an 870-day period sinusoidal variation, have amplitudes and phases which vary with height and latitude. An analytical technique based on a Markov chain process is used to ensure proper horizontal and vertical correlations of the random perturbations.

2. Description of the model

a. The Jacchia section (above 90 km)

The Jacchia (1970) model for the thermosphere and exosphere was originally implemented to compute atmospheric density at satellite altitudes. The Jacchia model is made up of a set of analytical equations which can be evaluated at any desired height, latitude, longitude and time. The Jacchia model evaluates temperature and density variations due to solar and geomagnetic activity, diurnal and semi-annual variations, and seasonal and latitudinal variations.

b. The 0–25 km section

The 0–25 km atmospheric model, developed by Environmental Research and Technology (Spiegler and Fowler, 1972) was designed to extract from data tapes and interpolate on latitude and longitude, mean monthly and daily variance profiles of pressure, density and temperature at 1 km intervals from the surface to a height of 25 km for any location on the globe. The data tapes contain empirically determined atmospheric parameter profiles at a large array of locations. The Northern Hemisphere grid array is equivalent to the National Meteorological Center (NMC) grid network. Grids spaced at 5° intervals of latitude and longitude are used in the equatorial and Southern Hemisphere regions.

c. The modified Groves section (25–90 km)

The starting point for the middle atmosphere (25–110 km) is the latitude dependent model of Groves (1971). This empirical model combines many observations from a wide range of longitudes. Observational results over approximately six years were used to compute zonal averages (i.e., averages over longitude), which are presented versus latitude and month. Latitude coverage of the Groves model is from the equator to 70° or in some cases 80°. In order to overcome the difficulty of the lack of Groves values at 80° and 90° an interpolation scheme was used which was based on an assumed parabolic variation of the zonal mean values across the poles. Southern Hemisphere data were utilized in developing the Groves model as Northern Hemisphere data with a 6-month change of date. Inter-hemispheric differences are recognized (see, e.g. Labitzke, 1974; Belmont *et al.*, 1975). However, lack of Southern Hemispheric data in the 30–90 km height range forced this assumption to be retained. The 0–25 km height range (where most of the topographic influence will be felt) is handled by separate Northern and Southern Hemisphere data in that section of the program. When the Southern Hemisphere data base in the 30–90 km height range becomes adequate, this atmospheric region can also be treated separately in the atmospheric model program. The Groves model data has only height and latitude variation for each month. Since longitude variation was required, the Groves model data had to be modified to incorporate this additional variation. Unfortunately, the Groves region (25–110 km) is data-sparse, and most of the available data have already been used by Groves in the development of his model. A scheme for using 10, 2 and 0.4 mb map data and extrapolating up to 90 km was devised for purposes of evaluating longitude dependent relative deviations from the Groves data. These deviations, called *stationary perturbations*, were evaluated at longitudes 10°, 40°, 70°, ... 340° for latitudes 10°, 30°, 50°, 70°, 90°. The stationary perturbations at heights of 30, 40 and 52 km were evaluated from data read from 10, 2 and 0.4 mb upper air charts. Presently these results are averages from the 1966 and 1967 10 mb charts (NOAA, 1969b) and the 1966, 1967 and 1968 2 and 0.4 mb charts (NOAA, 1969a, 1970, 1971). The only other currently available charts [for 1964 and 1965 and more recently for 1972 and 1973 (NASA-SP-3091)] are now being read to improve the modeling of the stationary perturbations. Lack of 2 and 0.4 mb chart data over portions of the eastern hemisphere meant that these charts had to be subjectively extrapolated to fill the data gap. Comparisons of model results with Russian meteor winds at 90 km indicate, however, that no serious error resulted from this procedure. In order to introduce longitude variability at heights above 52 km, the extrapolation technique of Graves *et al.* (1973) was used to project the 52 km interpolated chart data up to 90 km. The five extrapolation height levels are 60, 68, 76, 84 and 90 km. Graves has shown this technique to give reasonable extrapolations to 90 km, and the simulations with the model (presented later in this paper) confirm the validity of the method. The Graves extrapolation method between 52 and 90 km is used in the model only to generate the longitude dependent stationary perturbations about the zonal means, with the zonal means still being taken from the Groves model. The 50–110 km region of the atmosphere is the most data-sparse, especially in the Southern Hemisphere and the eastern half of the Northern Hemisphere. Hence it is this region which can be improved most when the data base improves in this height range.

d. Winds in the model

Conceptually, an independent wind model, such as the east-west wind model of Groves (1971), could be added to the pressure, density and temperature model. However, the approach taken in the model was to compute a mean wind from the geostrophic wind equations (which rely on horizontal pressure gradients). The eastward (i.e., blowing toward the east) wind component u and northward component v can be evaluated from the geostrophic wind equations

$$u = -(1/\rho f)\partial p/\partial y, \tag{1}$$

$$v = (1/\rho f)\partial p/\partial x, \tag{2}$$

where ρ is the density, f the Coriolis parameter ($2\Omega \sin\varphi$), and $\partial p/\partial x$ and $\partial p/\partial y$ are the eastward and northward components of the horizontal pressure gradient. For evaluation in the model, the pressure gradient terms must be approximated by finite differences. Specific models for the random and quasi-biennial components of the wind are also added to the mean wind, as discussed later.

e. The random variations

In addition to the monthly means, two types of perturbation are considered in the model: random variations and quasi-biennial oscillations, discussed in the following section. The random variations are considered to have a Gaussian distribution about the monthly mean with a standard deviation σ determined from empirically observed atmospheric variability. Tables of the random pressure, density, temperature and wind components are input to the program from a data tape.

In the altitude range below 25 km the random σ's are taken directly from the data tapes as the square root of the tabulated variance values. For the region above 25 km, random σ's were evaluated (Justus and Woodrum, 1975) from Meteorological Rocket Network (MRN) and NASA grenade and pitot tube data summaries (Theon *et al.*, 1972), which covered 25 to 90 km. Above 90 km random σ's were estimated from previous study results (Justus and Woodrum, 1973) on atmospheric variation statistics. The random perturbation magnitudes in the thermodynamic variables were adjusted to make them consistent with constraints required by the perfect gas law (Buell, 1970) and the hydrostatic equation (Buell, 1972b). Vertical correlation scales for the random perturbations were evaluated (Justus and Woodrum, 1975) by Buell's (1972b) depth-of-pressure-systems equation and from vertical structure function analysis (cf. Justus and Woodrum, 1973). Use of the Buell depth-of-pressure-systems vertical scale for the random perturbations implies that profiles of pressure and density generated by the random perturbation model will have realistic vertical compensation, e.g., positive perturbations at some heights, negative at others. Horizontal correlation scales were evaluated from results of Buell (1972a) at the 500 mb (6 km) level, and from horizontal structure function analysis in the 25–130 km height range (Justus and Woodrum, 1973).

f. The correlated random perturbation model

The random perturbations to the monthly means are assumed to have a Gaussian distribution with a standard deviation determined as described above. However, to represent realistic perturbations, there must be correlation maintained between perturbations at successive positions along the profile or trajectory.

The random perturbation model used is an extension of one originally developed for simulation of turbulence (Justus, 1971; Justus and Hicks, 1971). The perturbations generated by the model are not only correlated with each other over successive times, but also a time series of such perturbations can be Fourier transformed and has a spectrum which agrees with that expected from the correlation function which describes the correlation between successive positions.

g. Quasi-biennial variations

In addition to the maximum near 25 km in the tropics, it was shown from periodogram analysis by Justus and Woodrum (1973) that quasi-biennial oscillations of the wind, pressure, density and temperature were significant in the height range 45–60 km. In many instances the amplitudes of the quasi-biennial oscillations were comparable to the annual and semiannual oscillations (e.g., near 45 km at low latitudes). Other publications have indicated the same (e.g. Belmont and Dartt, 1973; Cole, 1967; Rahmatullah, 1968). Consequently, in modeling the winds and thermodynamic variables of the atmosphere, the quasi-biennial oscillations should definitely be considered.

In the present work, the amplitudes and phases of the quasi-biennial oscillations were found by first performing harmonic analyses on MRN data from three sites. These results were combined with the previous results of Cole (1967), Rahmatullah (1968), Groves (1973), Shah and Godson (1966), Reed (1965) and Angell and Korshover (1962, 1963, 1964, 1965), and interpolated values of the quasi-biennial parameters were evaluated at the necessary latitudes throughout the height range 15 to 90 km. It was assumed in the above analysis that the quasi-biennial variations have no longitude dependence and are symmetric about the equator.

3. Sample results

The global reference atmospheric model program is designed to give two types of atmospheric parameters: values along a simulated trajectory, of which each position must be input to the program, and a profile (such as a vertical profile at a single location) for which the positions are automatically computed by the program after the initial position is given (any constant increments in height, latitude and longitude can be used).

Fig. 1 shows a ground plot of a "Mission 3" re-entry and return trajectory. Mission 3 has a 104° orbital inclination with launch from and return to Vandenburg AFB. The height and time along the trajectory ground plot are also shown in Fig. 1. Fig. 2 shows computed density, in percent deviation from the U. S. Standard Atmosphere, for a typical January run to simulate conditions along the return trajectory of Mission 3. The solid line and shaded area in Fig. 2 show the

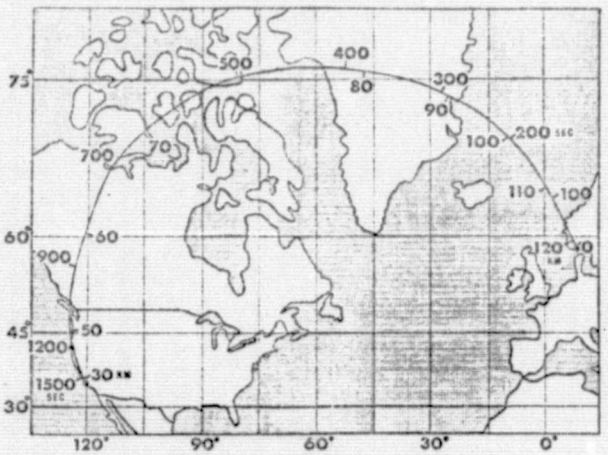

FIG. 1. Ground plot of the re-entry and return trajectory for Mission 3, a 104° inclination polar orbit launched from and returning to Vandenburg AFB. The altitude (km) is plotted on the inner side of the orbital plot and the time (s), measured from time of de-orbit, on the outer side.

monthly mean and ±2 standard deviations of the random density perturbations. The data points with error bars at 80 km height show observed mean and ±2 standard deviations at 80 km above Point Barrow, Alaska (Theon *et al.*, 1972), which is located at 71°N, 157°W some 5° south and 109° west of the 80 km height point on the trajectory. This polar orbit trajectory is the situation for which the model is most valuable, because of the large variations from nominal (1962 U. S. Standard) values which can be encountered.

Figs. 3–6 illustrate example applications of the model program and show the accuracy with which it is capable of reproducing actual atmospheric processes. Figs. 3a and 3b show quasi-meridional temperature cross sections through Point Barrow (71°N, 157°W), Fort Churchill (59°N, 94°W), Wallops Island (38°N, 75°W), and Natal-Ascension (6°S, 35°W and 8°S, 14°W). Fig. 3a was evaluated by the model from January and July runs for these four locations. Fig. 3b was evaluated by Theon *et al.*, (1972) from average summer and winter grenade and pitot tube data. Fig. 4 shows time cross sections of monthly mean temperature (°K) for Wallops Island (38°N). Fig. 4a was computed from 12 monthly vertical profiles evaluated by the atmospheric model program, and Fig. 4b was constructed by Theon *et al.*

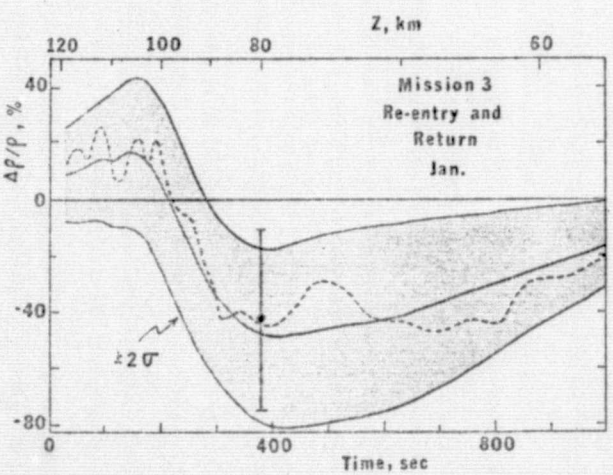

FIG. 2. Density along a January Mission 3 rentry and return trajectory. Density deviations are with respect to the 1962 U. S. Standard Atmosphere. The solid line and shaded area shows the January monthly mean and ±2 standard deviations of the random density perturbation. The dashed line shows a typical density profile of mean plus random component.

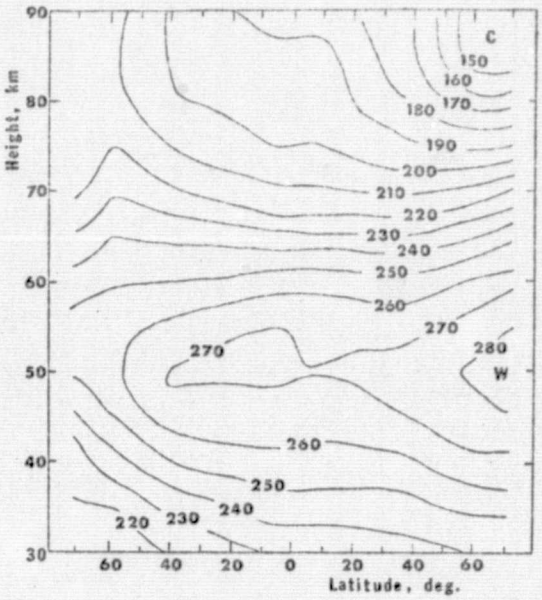

(a)

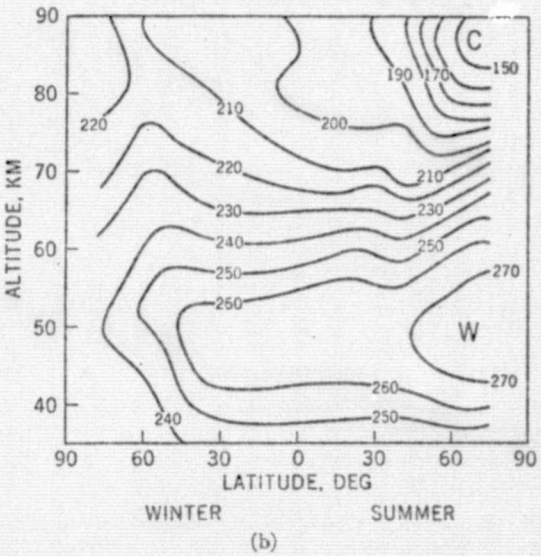

(b)

FIG. 3. Quasi-meridional cross section of temperature (K) for mean winter conditions at Point Barrow, Fort Churchill, Wallops Island, and Natal-Ascension: (a) computed by the model, and (b) observed by Theon *et al.* (1972).

(1972) from monthly mean profiles based on 93 rocket grenade soundings. Fig. 5 shows the average winter (December, January, February) circulation at 70 km. Fig. 5a was evaluated by averaging model calculated monthly means of pressure and winds, for the three winter months, and Fig. 5b was constructed by Theon *et al.* (1972) from 70 km observed winds and pressures at the locations indicated, and calculation of isobar orientation and spacing by the geostrophic wind equation. The good correspondence between Figs. 4a and 4b and between Figs. 5a and 5b indicates that no serious errors were introduced by the use of the Groves extrapolation of stationary perturbations in the 52–90 km height region. Fig. 6 shows similar winter circulation maps for 90 km in the eastern hemisphere. Fig. 6a was evaluated from the global reference atmospheric model, and Fig. 6b represents average observed winds at 90 km by the meteor wind method (Lysenko *et al.*, 1969). The nine lettered dots in Fig. 6b are meteor observation sites and arrows from these dots represent direction and speed of the diurnally and monthly averaged wind (scale of arrows not given by Lysenko). Arrows from non-lettered dots are hypothetical circulation patterns proposed by Lysenko for the period of observation (December 1965–January 1966). The comparisons in Figs. 3–6 indicate that the agreement between observed and model-computed atmospheric height, latitudinal, longitudinal and seasonal

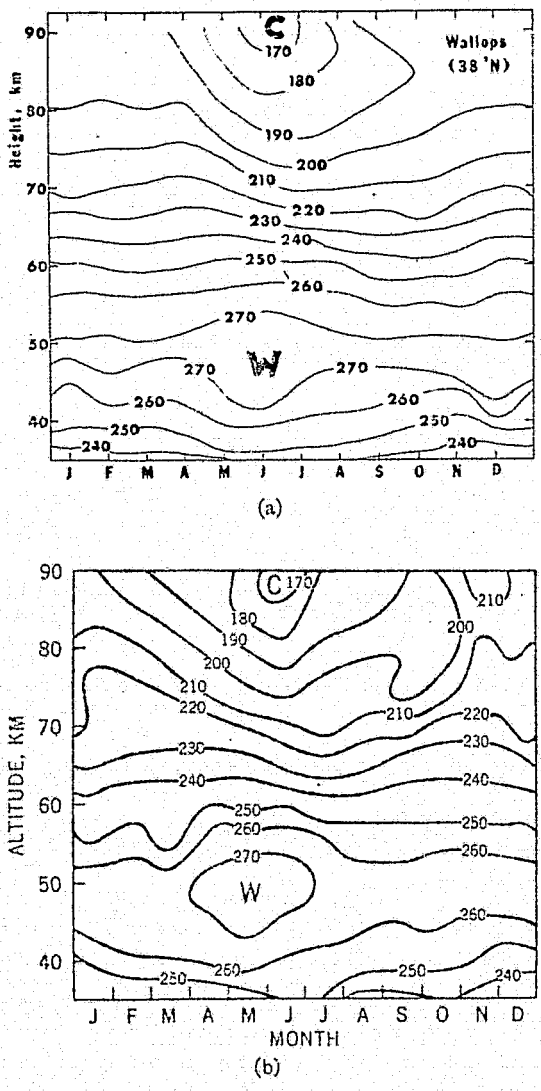

FIG. 4. Time cross section of monthly mean temperature (K) for Wallops Island (38°N) constructed from 12 monthly profiles: (a) evaluated by the model, and (b) observed by Theon *et al.* (1972).

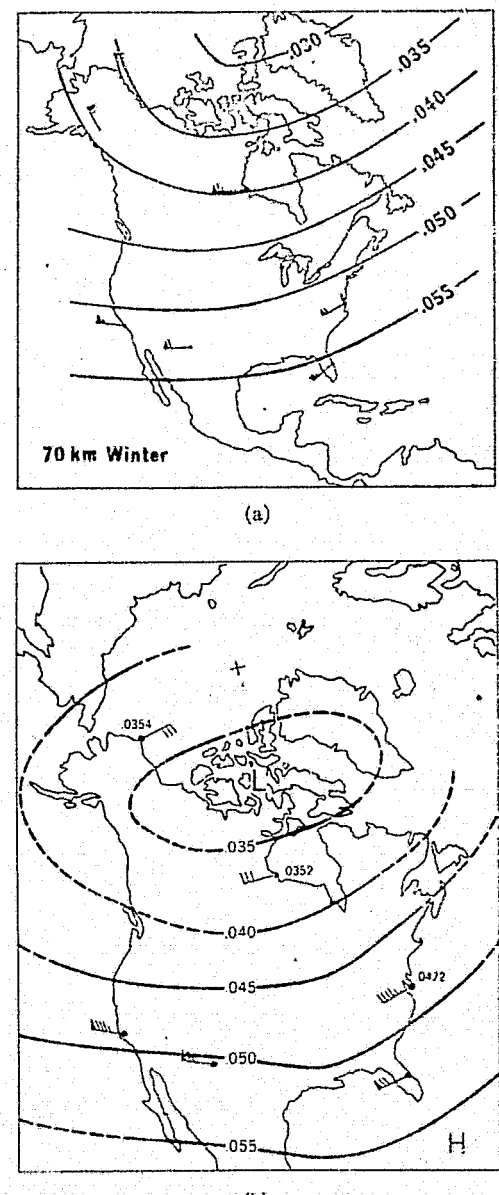

FIG. 5. Mean winter circulation at 70 km showing isobars (mb) and winds (m s^{-1}): (a) for the model [3-month (December, January, February) average] and (b) observed by Theon *et al.* (1972).

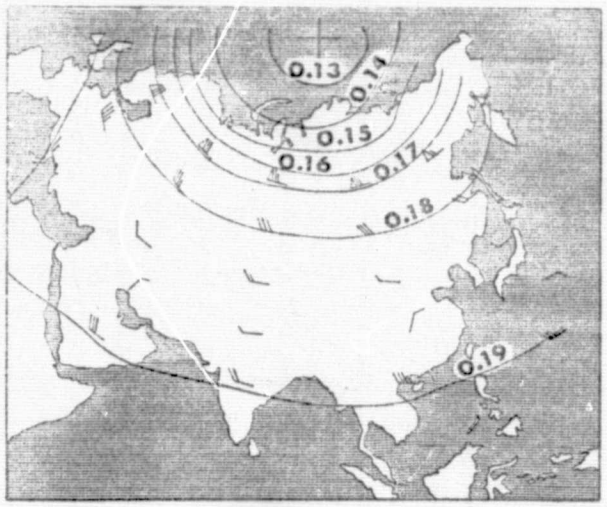

(a)

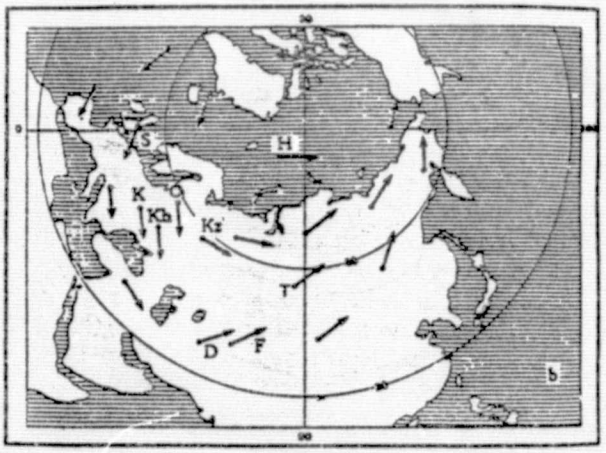

(b)

FIG. 6. Mean winter circulation showing isobars (N m^{-2}) at 90 km over Eurasia and the Arctic (a) as evaluated by the model, and (b) observed by Lysenko *et al.* (1969) from meteor wind measurements.

variations are quite good. The good correspondence between Figs. 6a and 6b indicates that no serious errors were introduced by the subjective extrapolations used to fill in the data gaps between 50 and 90 km above Eurasia.

Acknowledgments. Work on development of the global reference atmospheric model was performed under NASA Contract NAS8-29753, administered through the Aerospace Environment Division (AED) of Marshall Space Flight Center, William W. Vaughan, Chief. Thanks also go to Mr. Robert E. Smith (AED) for his assistance on the Jacchia model. The Jacchia model deck was originally supplied to us by R. L. King of Northrop Services, Huntsville. We also wish to thank Mr. M. E. Graves, also of Northrop Services, who provided advice on how to adapt his mesospheric extrapolation model. Mr. Dale Johnson (AED) has been most helpful in providing copies of the 4-D (0–25 km) data tapes, and Ms. Billie Robertson of the MSFC computer facility has been of great help in the computer liaison; these efforts are also appreciated. Special thanks to John Theon for providing originals for Figs. 3b, 4b and 5b.

Work on the global circulation simulations with the model is sponsored under NASA Grant NGL-11-002-004. Copies of the NASA technical memoranda (Justus *et al.*, 1974), describing the model program, are available upon written request to the authors.

REFERENCES

Angell, J. K., and J. Korshover, 1962: The biennial wind and temperature oscillations of the equatorial stratosphere and their possible extension to higher latitudes. *Mon. Wea. Rev.*, 90, 127–132.

——, and ——, 1963: Harmonic analysis of the biennial zonal-wind and temperature regimes. *Mon. Wea. Rev.*, 91, 537–548.

——, and ——, 1964: Quasi-biennial variations in temperature, total ozone, and tropopause height. *J. Atmos. Sci.*, 21, 479–492.

——, and ——, 1965: A note on the variation with height of the quasi-biennial oscillation. *J. Geophys. Res.*, 70, 3851–3856.

Belmont, A. D., and D. G. Dartt, 1973: Semiannual variation in zonal wind from 20–65 km, at 80°N-10°S. *J. Geophys. Res.*, 78, 6373–6376.

——, ——, and G. D. Nastrom, 1975: Variations of stratospheric zonal winds, 20–65 km, 1961–1971. *J. Appl. Meteor.*, 14, 585–594.

Buell, C. E., 1970: Statistical relation in a perfect gas. *J. Appl. Meteor.*, 9, 729–731.

——, 1972a: Correlation functions for wind and geopotential on isobaric surfaces. *J. Appl. Meteor.*, 11, 51–59.

——, 1972b: Adjustment of some atmospheric statistics to satisfy physical conditions. *J. Appl. Meteor.*, 11, 1299–1304.

Cole, A. E., 1967: Periodic oscillations in the tropical and sub-tropical atmosphere at levels between 25 and 90 Km. *Space Research VIII*, Amsterdam, North Holland Publ. Co., 823–834.

Graves, M. E., Y. S. Lou and A. H. Miller, 1973: Specification of mesospheric density, pressure, and temperature by extrapolation. NASA CR-2223.

Groves, G. V., 1971: Atmospheric structure and its variations in the region from 25 to 120 km. AD-737 794, AFCRL-71-0410, Environ. Res. Pap. No. 368.

——, 1973: Zonal wind quasi-biennial oscillations at 25–60 km altitude, 1962–1969. *Quart. J. Roy. Meteor. Soc.*, 99, 73–81.

Jacchia, L. G., 1970: New static models of the thermosphere and exosphere with empirical temperature profiles. *Smithsonian Astrophys. Obser., Spec. Rept.*, No. 313.

Justus, C. G., 1971: Computer modeled diffusion in stratified shear flow. Presented at the Amer. Geophys. Union Meeting, Washington, D. C., April.

——, and J. E. Hicks, 1971: Modeling the anisotropy in stratified shear flow. *Proc. Symp. Air Pollution, Turbulence and Diffusion*, Las Cruces, N. M., Sandia Laboratories, 202–207.

——, and A. Woodrum, 1973: Short and long period atmospheric variations between 25 and 200 km. NASA CR-2203.

——, and ——, 1975: Revised perturbation statistics for the global scale atmospheric model. NAS8-30657.

——, R. G. Roper, and O. E. Smith, 1974: A global scale engineering atmospheric model for surface to orbital altitudes. NASA-TM-X 64871 (Technical Description) and NASA-TM-X-64872 (Users Manual and Programmers Manual).

Labitzke, K., 1974: The temperature in the upper stratosphere—differences between hemispheres. *J. Geophys. Res.*, 79, 2171–2175.

Lysenko, I. A., B. L. Kashcheyev, K. A. Karicemov, M. K. Nazarenko, A. D. Orlyanskiy, Ye. I. Fialko and R. P. Chebotarev, 1969: Results of radar-meteor tracking studies on atmospheric circulation over Eurasia and the Arctic. *Izv. Atmos. Oceanic Phys.*, 5, 508–513.

NOAA, 1969a: Weekly Synoptic Analyses, 5, 2, and 0.4 Millibar Surfaces for 1966. WB 9, Staff, Upper Air Branch, NOAA, NMC.

——, 1969b: Monthly Mean 100, 50, 30, and 10 Millibar Charts and Standard Deviation Maps, 1966–1967. WB 11, prepared by the Staff, Upper Air Branch, NOAA, NMC.

——, 1970: Weekly Synoptic Analyses, 5, 2, and 0.4 Millibar Surfaces for 1967. NWS, 14, Staff, Upper Air Branch, NOAA, NMC.

——, 1971: Weekly Synoptic Analyses, 5, 2, and 0.4 Millibar Surfaces for 1968. NWS, 14, Staff, Upper Air Branch, NOAA, NMC.

Rahmatullah, M., 1968: Quasi-biennial oscillation and atmosphere structure in the stratosphere and mesosphere. *Space Research VIII*, Amsterdam, North Holland Publ. Co., 761–781.

Reed, R. J., 1965: The quasi-biennial oscillation of the atmosphere between 30 and 50 km over Ascension Island. *J. Atmos. Sci.*, 22, 331–333.

Shah, G. M., and W. L. Godson, 1966: The 26-month oscillation in zonal wind and temperature. *J. Atmos. Sci.*, 23, 786–790.

Spiegler, D. B., and Mary G. Fowler, 1972: Four-dimensional world-wide atmospheric model—Surface to 25 km altitude. NASA CR-2082.

Theon, J. S., W. S. Smith, J. F. Casey and B. R. Kirkwood, 1972: The mean observed meteorological structure and circulation of the stratosphere and mesosphere. NASA TR R-375.

TURBULENCE IN THE LOWER THERMOSPHERE

by

R. G. Roper
School of Aerospace Engineering
Georgia Institute of Technology
Atlanta, Georgia 30332

A static, or motionless, atmosphere can be adequately described on a macroscopic scale by three parameters - its pressure, temperature and density. On a molecular scale, its mean molecular weight, the weight of a hypothetical average molecule, becomes important. For a gas to exert pressure, its molecules will have a velocity proportional to the square root of the gas temperature. The real atmosphere is composed of several species, nitrogen, oxygen, carbon dioxide, argon, helium and hydrogen, for example, and for a given macroscopic state each specie will have a velocity inversely proportional to its molecular mass. If the real atmosphere were macroscopically motionless (its molecules in purely random motion) one would find a decrease in mean molecular weight with altitude - the lighter species would separate from the heavier species by the process of molecular diffusion. Such a process is not observed in the Earth's atmosphere until one reaches an altitude of from 100 to 110 kilometers - up to this altitude the mean molecular weight remains approximately constant. This comes about because the Earth's atmosphere is not motionless on a macroscopic scale, but is continually being mixed by atmospheric turbulence. The commencement of diffusive separation at 100-110 kilometers does not mean that there are no winds to cause turbulence and mixing at these altitudes, but rather that, at such low densities, molecular diffusion rates become much greater than

wind induced mixing rates. This article concentrates on the region known as the lower thermosphere, between the mesopause at approximately 80 kilometers, where the atmosphere is always mixed, and the altitude of 130 kilometers where diffusive separation is always observed.

Our knowledge of mixing processes in the upper atmosphere has been accumulated in the years post World War II. While the lower thermosphere has been probed using for decades radio techniques, detailed knowledge of its structure has only come with the use of rocket soundings.

Before considering the techniques of measurement of mixing processes in the upper atmosphere, and the interpretation of those measurements, a definition of "mixing process" is pertinent. On a global scale, the atmosphere can be said to be mixed by the transport of constituents from one location to another by large scale wind systems. This "mixing" is very important - important enough to warrant a separate chapter in this book (Roble: Chapter 3). Here, however, we will concern ourselves with more localized mixing, usually brought about in the free atmosphere by shears in the wind system, and called atmospheric turbulence. A turbulent atmosphere is mixed at a rate hundreds or more times faster than its molecules can statically diffuse, and thus turbulence will maintain homogeneity in an atmosphere composed of several molecular species. Hence the term "homosphere", often applied to describe the homogeneous atmosphere, with the "heterosphere" above. The level at which mixing ceases has been referred to as the "homopause", but we will use the term "turbopause".

In addition to mixing the atmosphere, locally intensive turbulence will also cause local heating. Turbulence is dissipative, extracting energy from the total flow, and transferring it by a cascading process

to scales so small that the random motion of the molecules, which determines the temperature, is increased. Thus turbulence in the lower thermosphere is important because its intensity affects the relative concentrations of the constituents of the thermosphere, and the heat budget in the neighborhood of the mesopause. Since the source of the turbulent energy resides in the lower atmosphere, and this energy is transferred to the thermosphere by the upward propagation of internal atmospheric gravity waves and tidal winds (Hook: Chapter 8), a detailed knowledge of the behavior of the turbopause enables specification of one of the primary energy sinks required by meteorologists for the formulation of global models of the lower atmosphere.

Introduction

In the parlance of ionospheric physicists, the lower thermosphere as defined here is known as the E region. The E region has been probed from the ground almost since the inception of radio. In particular, "irregularities" in the structure of the ionization producing reflections at this altitude have been observed for decades. Because these irregularities could be observed only through reflection from the continually changing ambient ionization imbedded in the neutral atmosphere, their interpretation in terms of the turbulent structure of the neutral atmosphere was highly speculative. However, in the early 1950's, a technique was devised which enables the characteristics of the neutral atmosphere to be determined by direct observation of relatively well understood radio reflectors - the ionized trails formed by meteors entering the Earth's atmosphere.

Measurements of the radio frequency doppler shifts produced as meteor trails were blown along by the neutral winds between 80 and 100 km (the alti-

tude range over which most meteors "burn up" in the Earth's atmosphere) were (and still are) used to provide knowledge of the neutral wind and its variation in both height and time. At the same time, considerable progress was being made by scientists working in the analysis and interpretation of atmospheric turbulence in the troposphere. The interpretation was assisted in no small measure by the progress being made in turbulence theory, in particular by Batchelor's "Theory of Homogeneous Turbulence" (1953). After this theory was applied successfully to the explanation of the scattering by the tropospheric atmosphere of very high frequency radio waves, Booker and Cohen (1956) attempted to explain the fading observed on long duration meteor echoes in terms of turbulence in the neutral atmosphere at E region altitudes. From their data, they deduced that energy was being extracted from the large scale wind motions at meteor altitudes and dissipated at a rate $\varepsilon = 25$ watts/kg . While the underlying theory was sound, their paper was attacked on the basis of their interpretation of the echo fading process.

In the late fifties, the chemical release rocket technique was perfected, and used to introduce a visible tracer, initially sodium, into the atmosphere over the altitude range 80 to 200 kilometers. Such a release, made at twilight, so that the trail was illuminated by sunlight while the ground was in darkness, could be photographed from several camera sites on the ground, and the time series of exposures simultaneously recorded could be used for triangulation of the release, and its motion with time. Thus winds could be determined for as long as the trail remained visible - sometimes for as long as 15 minutes. Since the early sixties, tri methyl aluminum (TMA), which reacts with the ambient atmosphere to produce products which not only scatter sunlight, but also glow in the dark (making night time as well as twilight measurements possible) has been

used, as well as sodium and, for daylight releases in particular, lithium.

One outstanding feature of these trails is the fact that below an altitude of some 105 kilometers the release is "obviously turbulent", while above that altitude the trail expands smoothly, as it would under the action of molecular diffusion alone. Considerable controversy still exists over the interpretation of data from rocket released vapor trails as evidence for turbulence of the ambient atmosphere. Some interpretations of sodium vapor trails, for example, have lead to anomalous results, which are thought to be related to the energetics of the thermite burn necessary to produce the sodium vapor. However, interpretation of the breakup of vapor trails, below what has become known as the turbopause, is not the only evidence for the existence of turbulence at these altitudes. Theoretical studies of the atmospheric heat budget in the high atmosphere by Johnson and Gottlieb (1970), for example, require vertical diffusivities below the turbopause what are much larger than molecular; calculations of the diffusivities responsible for the measured constituents above the turbopause also require similar high values of diffusivity below the turbopause; composition measurements made using rocket borne mass spectrometers show the level of diffusive separation to be considerably higher than would be the case in a non turbulent atmosphere, and a completely different class of measurements, based on the shearing of radio meteor trails by the winds in the 80 to 100 km region (rather than the fading of individual meteor echoes), yields values consistent with those deduced from vapor trail observations.

The Interpretation of Measurements

Is it possible for wake effects and chemical energy released in contaminants to influence the subsequent dispersion? Certainly - such effects have

been documented. For energetic releases, such as rocket burn and large quantities of explosive, the "release phase" at thermospheric altitudes lasts only for some ten seconds or less. Figures 1 and 2 show an excellent example of a release phase anomaly in a TMA trail, as photographed by the Smithsonian Institution's Baker Nunn camera at Woomera, Australia (31° S). Figure 1 shows a portion of trail two seconds after release in the 100 to 110 km height range. The "vortex shedding" on the right hand side of the trail is clearly visible. In figure 2, a frame taken four seconds later, the effects of this motion have disappeared. The subsequent breakup of the trail, with the production of the characteristic "obviously turbulent" appearance, did not occur until some thirty seconds later, as illustrated in the isodensitrace montages of Figure 3. These unique Baker Nunn photographs are an example of the rewards of international cooperation. The Smithsonian Institution for many years operated a world wide network of Baker Nunn cameras for the photographic determination of satellite positions. Relationships between the satellite station staff and the Australian and British rocket experimenters at Woomera were such that the Baker Nunn would be used to photograph the rocket releases, when such use did not interfere with the primary mission of the observatory.

The abrupt cutoff in ambient turbulence (the turbopause), which almost always underlies a region of high wind shear, is illustrated in Figure 4. That the breakdown from "obviously laminar" to "obviously turbulent" represents a dramatic change, easily recognized by visual inspection of the film, is shown in Figure 5, in which the square of the effective radius of the trail is plotted against time after release at 105 km. The growth in the first few seconds after release is an order of magnitude faster than the subsequent growth up to the time of trail breakup, and this is regarded as representing the re-

lease phase, in which the energetics are definitely non-ambient. The growth between 8 and 32 seconds after release could be molecular diffusion of a cloud with an initial radius of 130 meters, i.e. the release produced a cloud with, effectively, this radius at zero time. However, one can only say that the growth during this phase could be molecular - the 15% error in the determination of the effective radius from each film frame, and the fact that the trail cross section is only approximately Gaussian, precludes a measurement of diffusion coefficient to better than a factor of three. The onset of turbulence occurs 33 seconds after release, and then proceeds to follow the dispersion relation predicted by the theory of homogeneous turbulence

$$r_e^2 \alpha t^3$$

until, at 54 seconds, the trail becomes too irregular for an estimate of radius based on a Gaussian distribution to be meaningful. However, Figure 5 does provide two parameters (the effective radius at transition, and its time of occurrence after release) which should characterize the small scale end of the turbulence spectrum.

The most important parameter of any turbulence spectrum is ε, the rate of dissipation of turbulent energy. In order to calculate ε from any set of space/time correlations, it is necessary to use a model. The simplest is that of A. Kolmogoroff, as elaborated on by Batchelor (1953). Kolmogoroff put forward the hypothesis that, in any turbulent flow field in which energy was being extracted from the large scale or mean motion and cascaded to smaller scales before eventual dissipation at scales where molecular viscosity becomes important, there could exist a range of scales sufficient removed for the large scale, anisotropic eddies, and yet not appreciably damped by molecular viscosity, which would be both homogeneous and isotropic. The assumptions of

homogeneity and isotropy inherent in this model are open to question in the case of lower thermospheric turbulence, but a considerable amount of work by several experimenters has shown these assumptions to be reasonable, at least for length scales less than 1 km.

Batchelor (p.115, 1953) defines the basic length parameter of the viscous dissipation (small scale) region as

$$\eta = \left(\frac{\nu^3}{\varepsilon}\right)^{1/4}$$

where ν is the kinematic viscosity (a measure of molecular diffusivity), and η is in meters/radian.

Batchelor (p.150, 1953) also defines this unit length scale in terms of a characteristic time constant t^* such that

$$\eta = (\nu t^*)^{1/2}$$

Combining these two equations to eliminate η yields

$$t^* = \left(\frac{\nu}{\varepsilon}\right)^{1/2}$$

In terms of the length scale η,

$$\varepsilon \propto \eta$$

In terms of the time scale t^*,

$$\varepsilon \propto t^{*-2}$$

Wind shear results have been previously used to calculate the variation with height, z kilometers, of the rate of dissipation of turbulent energy ε (Roper 1966b). The kinematic viscosity ν may be determined from the viscosity and

density published in the U.S. Standard Atmosphere Supplements (1966). The function

$$\nu(\text{meters}^2\ \text{sec}^{-1}) = \exp[0.17\ (z - 80.0)]$$

with z in kilometers, has been found to fit the data at the tabulated altitudes, and was used to compute ν at 1 km height intervals. This ε profile is shown in Figure 6, together with the more directly measured profile of Justus (1967), calculated from the velocity fluctuations observed on 18 TMA trails. These values of ε and ν have been coupled to produce what can be regarded as average height dependent characteristic length scales η_R (= $2\pi\eta$ above, in order to express the length scale in the more usual wavelength notation, meters/cycle) and time scales t_R^*. These are plotted, together with η_J and t_J^* calculated from Justus' ε profile, in Figures 7 and 8 respectively. Also plotted are the values of η and t* determined from two Skylark released TMA trails photographed by the Baker Nunn camera at Woomera at dawn and dusk on May 31, 1968.

The similarity in form, and the order of agreement, between the predicted "average" trail time constants t_R^* and t_J^* and the measured values for each of the two releases is surprisingly good when one considers the approximations involved in

a) the model atmosphere viscosity, which is at best approximate above 80 km;

b) the variation, both diurnal and seasonal, in the turbulent dissipation rate, which has been averaged out in the construction of the t_R^* and t_J^* profiles and

c) the fact that, while the parameter t* appears to be a measure of the time taken for trail breakup to occur, it is not clear why it should be.

The definition of η is a mathematical expedient characterizing the spectrum of scales responsible for the viscous dissipation. There is no obvious

reason why either η or t^* should be physically measurable features of the motion. Nevertheless, the close similarity in the shapes of the t^* curves strongly indicates that the time delay in the onset of turbulence should be related to the time constant of the Kolmogoroff microscale. Furthermore, these observations suggest a reason why the turbopause, defined as the boundary between the regions which break up and which remain laminar, should manifest itself so abruptly. Above 105 km the time constant t^* for the onset of turbulence increases so rapidly with altitude that the trail is not, in general, observed for a sufficient length of time for visible breakdown to occur.

Attempts have been made to explain the existence of the turbopause in terms of a critical value of some parameter, generally the Reynolds number Re or the Richardson number Ri. These attempts have met with marginal success, partly because of the difficulty in defining the characteristic lengths which occur in these parameters, partly because it is not evident, a priori, what value the parameter should have at the turbopause. Without a detailed knowledge of the temperature gradient at the scale characteristic of the vertical mixing process (a few hundred meters or less) the Richardson number just cannot be specified. Johnson (1975) has considered the relative importance of buoyancy and dissipation in detail, referring particularly to the work of J. D. Woods, who determined that there was hysteresis in the onset criterion - laminar flows become turbulent when $Ri \leq 0.25$, while turbulent flows become laminar when $Ri \geq 1$. While the mean (undisturbed) atmospheric temperature profile is pertinent to the breakdown from laminar to turbulent flow, once turbulence is established its cessation will depend on the temperature gradient as modified by the turbulence. As yet, there is no technique available for measuring such temperature gradients in the lower thermosphere.

Another error which has often been made in attempting to explain turbulence in the lower thermosphere, is the assumption that the turbopause corresponds to an altitude at which turbulence ceases abruptly. The results presented here, on the contrary, show that the turbopause is the altitude at which the time constant of the Kolmogoroff microscale of the turbulence increases very rapidly with altitude. This viewpoint resolves the paradox that regions above the turbopause, which were thought of as non-turbulent, have a diffusion coefficient based on the measured laminar trail growth which is greater than molecular. We now see that turbulence does exist above the turbopause, but that its efficacy in transport processes relative to molecular diffusion, decreases with altitude. At a mean altitude of 130 km, the contribution of turbulence to diffusivity is insignificant, even though its absolute value may be as large as it is at the turbopause.

The rate of dissipation of turbulent energy may also be calculated from η, the length scale at which eddy diffusion becomes effective. However, since this length depends critically on the shape of the cloud (the assumed Gaussian variation across the cloud is rarely realized, in practice, below the turbopause) and because $\varepsilon \propto \eta^{-4}$, Rees et al (1972) chose to use the relatively precisely determined t^* values to calculate the variation of ε with height. This is shown, for a pair of dawn and dusk releases above Woomera (30° S) on May 31, 1968, in Figure 9. Note that the turbopause is higher in the evening than in the morning, and that the higher turbopause is associated with a greater overall turbulent intensity. This substantiates the suggested variation in midlatitude turbopause height made by Elford and Roper (1967), which was based on seasonal variations in turbulent intensity at 93 km, as determined from the wind shear measured simultaneously on individual radio meteor trails.

Also presented here are the results from two further TMA releases, made above Woomera at dawn on October 16, and dusk on October 17, 1969 (Figure 10). For this pair of trails, the turbulent intensity is higher in the morning than in the evening - opposite to the May 1968 releases. This diurnal variation with season is the same as that measured for the large scale turbulent velocity component from radio meteor winds at Adelaide (35° S). These October releases are of particular interest, in that they show alternating laminar and turbulent regions similar to those previously reported by Blamont and Barat (1967). The various layers observed in these releases do not seem to be quite as simply related to the wind profile as those of Blamont and Barat. However, the regions of prolonged laminar behavior all seem to be located at altitudes where the wind shear is high.

In an attempt to explain why, at times, the turbulence in the lower thermosphere should be stratified, and, in fact, why an ostensibly highly stable region of the Earth's atmosphere should be turbulent at all, Lloyd et al (1972) proposed a model in which random internal atmospheric gravity waves produced turbulence accompanied by a considerable modification of the mean temperature profile. The creation of temperature inversions by turbulence is commonplace in the troposphere because of the less stable mean lapse rate. It is proposed that a similar effect occurs in the more stable lower thermosphere, with part of the vertical component of the gravity wave velocity as the source of the turbulent energy.

If random, internal atmospheric gravity waves are propogating at a significant angle to the vertical, then their vertical velocity component will be able to contribute to the destabilization of the stably stratified lower thermosphere (Hodges, 1967). Similar destabilization mechanisms have been discussed

for the oceans by Phillips (1971), and for the lower stratosphere by Roach (1970). Radio meteor studies have already established that the gravity wave spectrum is the source of the turbulent energy in the lower thermosphere. This has been confirmed, quite independently, by Spizzichino (1972), also from radio meteor studies, and by Blamont and Barat (1967) from observations of chemical releases.

The lower thermosphere is stabilized against vertical motion by the mean temperature gradient; above the mesopause at 80 to 90 kilometers the mean temperature increases with height. By equating the work done in the vertical displacement of a parcel of gas to the fraction of the vertical component of the gravity wave spectrum which is responsible for the measured turbulence spectrum, Lloyd et al deduced the modification of the mean temperature profile which would be produced by the turbulence measured on the October 16 trail in the height range 104 to 110 kilometers. An isodensitrace montage of this portion of the trail is shown in Figure 11. The choice of the turbulent layers within which the analysis can be applied is somewhat subjective, being based on regions where growth is "obviously" different from that above and below.

The solid lines of Figure 12 show the results of the application of the Lloyd et al model to each of the layers delineated in Figure 11. The dashed lines are necessary for profile continuity, and must represent laminar sheets. Because of the discontinuous nature of the determination of the modified profile, and the forced fitting of the mid point temperature, the magnitudes of the positive and negative gradients are open to question. However, it is interesting to note that the existence of similar gradients in the lower stratosphere, a region of similar mean temperature gradient, is well documented, as can be seen from the project HICAT determination of Figure 13 from Mitchell

and Prophet (1969). Unfortunately, the flight of an aircraft at constant altitude cannot reveal a height profile of turbulence, but at least in the encounter with CAT at 21 km, the temperature profile has been modified in a manner commensurate with the present model.

Several deficiences exist in the model since the finite time constants of the processes involved (the period of the destabilizing gravity wave, for example) have not been considered. The basic energy budget equation can be made more general by the inclusion of terms describing energy sinks (e.g. heat conduction). One promising model being developed uses the reversible heating associated with propagating gravity waves (Hines, 1965) as the initial destabilizing energy.

Even with this criticism, the above semi-empirical approach allows deduction of many reasonable properties of the atmosphere. In particular, the model counters the objections raised to the existence of turbulence in what ostensibly is a highly stable region, since the presence of turbulence itself tends to destabilization by modification of the temperature profile.

Up to this point, major emphasis has been placed on the fundamental parameter ε, the rate of dissipation of turbulent energy. There is an equally important, though not as easily defined parameter, K_z, the coefficient of turbulent eddy diffusion in the vertical, which is the transport parameter incorporated in all realistic models of the chemistry and constituents of the lower thermosphere. For some time, there was considerable discrepancy between the diffusion coefficients calculated from the growth of rocket released contaminants, and those inferred from measurements of diffusive separation and atmospheric heat budget calculations. With the discovery that the turbulence responsible for the enhanced diffusivity of chemical releases in the lower therm-

osphere was highly anisotropic, with horizontal scales ten times those of the vertical, this discrepancy was readily explained. Since the time constant t* for the observed onset of turbulence as used by Rees et al (1972) is characteristic of the small scale, isotropic turbulence spectrum, Lloyd et al (1972) used the ε values thus determined to estimate the vertical diffusion coefficient . By an extension of their temperature profile modification model, they equated the vertical destabilizing influence of the turbulence to the stabilizing influence of the mean temperature profile to give a vertical diffusion coefficient

$$K_z = \frac{\beta\varepsilon}{\frac{g}{T_o}\left[\frac{dT_o}{dz} + \Gamma\right]}$$

where g is the acceleration due to gravity, T_o is the mean temperature at the altitude z, $\frac{dT_o}{dz}$ is the undisturbed mean temperature gradient, and Γ is the adiabatic temperature lapse rate, 9° K per kilometer. The above relationship is based on the premise that as long as the vertical temperature gradient remains greater than the adiabatic, there is an inhibition of vertical transport by vertical motion. It is interesting to compare this relationship with that determined independently by Lilly et al (1973) for the lower stratosphere. The constant β above was determined from turbulence theory to be 10. Lilly arrived at the value of 1/3! This discrepancy is not as serious at it appears at first sight, since Lilly's temperatures and temperature gradients were the measured values, leading to a considerably smaller denominator than that produced by the use of the undisturbed mean temperature and gradient values by Lloyd et al. The variation of K_z with height for the October 1969 releases, is graphed in Figure 14. The theoretically deduced upper limit for eddy diffusion, based on the heat flux model of Johnson and Gottlieb (1970) is shown for comparison.

Note that the maximum value of eddy diffusivity estimated by Johnson and Gottleib is the integrated global maximum averaged over all seasons, and can be exceeded by a particular measurement if there is any latitudinal, diurnal or seasonal variation of K_z. Note also that all the turbulent intensity and diffusivity profiles presented here reflect the apparent sharp cutoff in turbulence as observed on chemical trails. With the time constant in onset of turbulence increasing so rapidly at and above the turbopause, most trails are not observable long enough for breakdown to occur. However, diffusivities between the turbopause and approximately 130 km are usually greater than molecular, in keeping with the Johnson and Gottlieb calculations.

To determine the effect of seasonal changes in the temperature profile on the vertical diffusivity, the U.S. Standard Atmosphere (1966) summer, winter, and spring/fall model temperature profiles were combined with the turbulent dissipation rate profile of Roper (1966b) shown in Figure 6 to produce the K_z profiles of Figure 15. While there are discernable differences between the profiles, these differences are so small compared to the measured diurnal variations observed (Figure 10 for example) that they can hardly be regarded as significant. The absolute magnitudes, being three times those of the Johnson and Gottlieb calculation, are probably too high - a consequence of the assumptions made in relating ε to K_z.

The only two sets of data so far produced which are ameanable to analysis in terms of month by month variation of ε or K_z have been determined from meteor trail shear measurements made at Adelaide (35° S) by Roper (1966a) and McAvaney (1970). The variation of the monthly mean K_z at 93 km is shown in Figure 16. Also plotted in this figure are the results deduced from a far more rigorous treatment of the 1961 ε data by Zimmerman (1973); some modifications of absolute

values is evident, but the overall variation, with equinoctial maxima, remains. There is a real difference between the 1961 and the 1969 data which is not one of location, interpretation or technique. The higher values measured in 1969 are probably a consequence of the higher solar activity that year.

Sources of Turbulence Energy

The fact that random internal atmospheric gravity waves are the source of the turbulence energy in the lower thermosphere has already been mentioned. While this subject is covered in detail elsewhere in this volume (Hook, Chapter 8), one further correlation is pertinent to this discussion. In looking for possible sources of the turbulence in the meteor region, comparisons were made with the magnitudes of the prevailing and tidal winds and shears as measured simultaneously by the radio meteor method. While no apparent relationship existed between the turbulence parameters and the prevailing and semidiurnal winds, the seasonal variation of the amplitude of the diurnal oscillation was highly correlated with the turbulent intensity. The monthly means of the amplitude of the diurnal tide for several years of observation are shown in Figure 17. Note that equinoctial maxima in the diurnal tidal wind amplitude are not observed in all years, and therefore that the measured variation in turbulent intensity may not be characteristic of all years.

The global scale diurnal tidal wind does not produce turbulence directly, but by a cascade process, in which the tidal wind becomes unstable and generates in situ a spectrum of random internal atmospheric gravity waves. This instability in the diurnal tidal wind may come about either because its amplitude becomes large, or because of non linear interaction with gravity waves generated below and propagating upward through the lower thermosphere. Such gravity waves propagating from below can themselves be a direct source of tur-

bulent energy. Thus the dominant feature of the turbulence in the lower thermosphere, even if it is present at all times, will be the intermittency of its intensity. Little is known of the role played by large scale motions, such as planetary waves, in the stability of this region of the atmosphere. In fact, since practically all measurements of turbulent intensity have been made at middle latitudes, the properties of the global turbopause, and the influence of the turbopause on, for example, the hemispherical asymmetries in minor constituents measured globally at satellite altitudes can hardly be estimated at this juncture. Our knowledge of the temperature structure of the turbopause region at scales less than 1 kilometer, which is crucial to the understanding of turbulence and diffusivity, is woefully inadequate. Present measurement techniques are quite incapable of such detail at these altitudes.

In addition to the modifications to the temperature profile already discussed, the dissipation of turbulent energy produces heating of the ambient atmosphere. For the mixed atmosphere of mean molecular weight 29, a rate of turbulent dissipation ε of 1 watt per kilogram produces heating of the ambient at the rate of 85° K per day. The top scale of Figure 6 gives the heating rates appropriate to the inferred turbulent dissipation rates. In the light of the considerable variability indicated by the measurements presented here, even more emphasis must be given to the rate of dynamical heating of the lower thermosphere, as proposed by Hines (1965). The dissipation of wind energy at these altitudes can, at times, give rise to local heating rates in excess of those due to solar input, which has usually been consiered the major source of heating in this region. The relative importance of turbulence in mixing and dynamical heating has been summarized by Johnson (1975).

Conclusions

While the turbulence in the lower thermosphere is isotropic to scales of a few hundred meters, the transition from the turbulence to the non dissipative scales of the gravity wave spectrum is gradual, and therefore horizontal diffusivity is greater than vertical diffusivity. Based on diffusivity criteria alone, one would say that the turbulence is anisotropic, with vertical scale of order 1 kilometer, and horizontal scale a few kilometers. The turbulent intensity is intermittent in both space and time, with large diurnal, and significant seasonal and possible solar cycle variations. For this reason alone, it is essential that simultaneously measured in situ values of atmospheric parameters should be used in any attempt at meaningful comparisons. Since practically all measurements of turbopause altitude and turbulent intensity have been made at middle latitudes, and those low and high latitude measurements that have been made have not been coordinated with simultaneous observations elsewhere, variations with latitude are largely unknown. However, it has been established by rocket grenade and falling sphere measurements that the winter polar mesopause is hotter than that at the summer pole, and that, in the absence of solar input, a significant atmospheric dynamical heating source is responsible. As has been shown, the turbulent dissipation of wind energy in the 90 to 125 kilometer height range is significant, and should therefore be included in any model of the thermospheric heat budget.

While knowledge of the vertical diffusivity in the lower thermosphere is vital to the understanding and modeling of thermospheric constituents, the role played by the global turbopause in the dynamics of the thermosphere has yet to be determined. High resolution photography, with a frame rate of at least one every two seconds, is able to produce data on turbulent intensities and vertical

diffusivities from rocket vapor trails, but is highly localized in time and space. A recent development, the use of a high flying aircraft as a camera platform, overcomes two ground based camera problems - atmospheric haze and clouds are avoided, and photographs can be taken in the daytime. Daytime releases of lithium can also be observed from the ground using narrow band filters and electronic scanning systems (recording on video tape), but interpretation of the dispersion of the highly energetic release in terms of turbulence parameters is difficult. Vertical diffusivities and turbopause altitudes can be inferred from rocket borne mass spectrometer measurements, regardless of hour of day or cloud cover, but with location limitations similar to the vapor trail method (both require reasonable range facilities). Multi-station meteor wind radars can provide a continuous measurement of the turbulent intensity just below the turbopause, but only a few stations, all in mid latitudes, are currently capable of this type of operation, and none do operate continuously. Incoherent scatter radars are able to measure the temperature structure in the neighborhood of the turbopause with about 2 kilometers height resolution, but are subject to constraints similar to, but even more severe, than those of the radio meteor technique. A suggestion by Bencze (1968) that an ionosonde can be used to measure turbopause altitude warrants further investigation, since a global network of ionosonde stations is already in existence.

A proper understanding of the nature of the turbulence in the lower thermosphere requires a knowledge of the temperature profile with better than 1 kilometer (preferrably 100 meters) resolution - a resolution which is not technically feasible at this time. Nevertheless, global variations in turbopause altitude and intensity can be determined using well established techniques, but only with international cooperation. Simultaneous global observations could be

coordinated through the Middle Atmosphere Program (MAP) of the International Association of Geomagnetism and Aeronomy, and the International Mesospheric and Ionospheric Structure Parameter Interaction program (MISPI) proposed by the Soviet Union. Particular emphasis is being placed by these programs on the encouragement of the artic, equatorial, southern hemisphere and antartic observations so badly needed for global coverage.

ACKNOWLEDMENTS

The writing of this paper was supported in part by the National Aeronautics and Space Administration under Grant NGL-11-002-004.

REFERENCES

Batchelor, G. K., "The Theory of Homogeneous Turbulence", Cambridge University Press, 1953.

Bencze, P., "An Analysis of the Virtual Height of Ionospheric Sporadic E($h'E_s$)," Acta Geodaet., Geophys. et Montanist. Acad. Sci. Hung., 5, 223-231, 1970.

Blamont, J. E. and J. Barat, "Dynamical Structure of the Atmosphere Between 80 and 120 Km", Aurora and Airglow, ed. by B. McCormac, Reinhold Publ. Co., p. 159, 1967.

Booker, H. G. and Robert Cohen, "A Theory of Long Duration Meteor Echoes Based on Atmospheric Turbulence with Experimental Confirmation", J. Geophys. Res., 61, 707, 1956.

Elford, W. G. and R. G. Roper, "Turbulence in the Lower Thermosphere", Space Res. VII, North Holland Publ. Co., Amsterdam, p. 42, 1967.

Hines, C. O., "Dynamical Heating of the Upper Atmosphere", J. Geophys. Res., 70, 177, 1965.

Hodges, R. R., Jr., "Generation of Turbulence in the Upper Atmosphere by Internal Gravity Waves", J. Geophys. Res., 72, 3455, 1967.

Johnson, Francis S., "Transport Processes in the Upper Atmosphere", J. Atmos. Sci., 32, 1658-1662, 1975.

Johnson, Francis S. and B. Gottlieb, "Eddy Mixing and Circulation at Ionospheric Levels", Planet. Space Sci., 18, 1707-1718, 1970.

Justus, C. G., "The Eddy Diffusivities, Energy Balance Parameters, and Heating Rate of Upper Atmospheric Turbulence", J. Geophys. Res., 72, 1035, 1967.

Lilly, D. K., D. E. Waco, and S. I. Adelfang, "Stratospheric Mixing Estimated from High Altitude Turbulence Measurements", Paper 73-497, AIAA/AMS Intern. Conf. Environmental Impact of Aerospace Operations in the High Atmosphere, Denver, 11-13, June 1973.

Lloyd, K. H., C. H. Low, B. J. McAvaney, D. Rees, and R. G. Roper, "Thermospheric Observations Combining Chemical Seeding and Ground Based Techniques - 1. Winds, Turbulence and the Parameters of the Neutral Atmosphere", Planet. Space Sci., 20, 761-789, 1972.

McAvaney, B. J., "Small Scale Wind Structure in the Upper Atmosphere", Ph.D. Thesis, University of Adelaide, Australia, 1970.

Mitchell, F. A. and D. T. Prophet, "Meteorological Analysis of Clear Air Turbulence in the Stratosphere", in Clear Air Turbulence and Its Detection, ed. Pao and Goldberg, Plenum Press, New York, p. 144, 1969.

Phillips, O. M. "On Spectra Measured in an Undulating Layered Medium", J. Phys. Ocean., 1, 1, 1971.

Rees, D., R. G. Roper, K. H. Lloyd, and C. H. Low, "Determination of the Structure of the Atmosphere Between 90 and 250 Km by Means of Contaminant Releases at Woomera, May 1968", Phil. Trans. Roy. Soc. London, A271, 631-666, 1972.

Roach, W. J., "On the Influence of Synoptic Development on the Production of High Level Turbulence", Quart. J. Roy. Meteorol. Soc., 96, 413, 1970.

Roper, R. G., "Atmospheric Turbulence in the Meteor Region", J. Geophys. Res., 71, 5785, 1966a.

Roper, R. G., "Dissipation of Wind Energy in the Height Range 80 to 140 Kilometers", J. Geophys. Res., 71, 4427, 1966b.

Spizzichino, A., "Wind Profiles in the Upper Atmosphere Deduced from Meteor Observation", in Thermospheric Circulation, ed. by Willis L. Webb, M.I.T. Press, Boston, 1972.

FIGURE CAPTIONS

Figure 1. Portion of a trimethyl aluminum trail showing a release phase instability with vortex shedding on the right hand edge 2 seconds after release.

Figure 2. As for Figure 1, but 6 seconds after release. Note that the release phase instability has been damped out.

Figure 3. Time history of a portion of the trail of Figure 2; showing the initial laminar behavior, and subsequent breakup induced by ambient atmospheric turbulence. Quantitative measurements of dispersion can be made from the isodensitrace contours.

Figure 4. Montage of the behavior of the trail above and below the turbopause.

Figure 5. Variation of the radius of the trail of Figure 1 with time after release at 105 km.

Figure 6. Profiles of the rate of dissipation of turbulent energy deduced from wind shears measured for 25 trails over Wallops Island (38° N)(Roper, 1966b), and from the dispersion of a similar number of trails over Eglin Air Force Base (29° N) by Justus (1967). The upper scale gives a measure of the atmospheric heating resulting from turbulent dissipation.

Figure 7. The variation with altitude of the Kolmogoroff microscales η_J and η_R inferred from the turbulent dissipation profiles of Figure 6. Also shown are the microscales inferred from the May 1968 trails. r_e^* is the Gaussian radius of the evening trail at t*, the time of onset of trail breakup.

Figure 8. The variation with altitude of the time constant of the Kolmogoroff microscale, for the ε profiles of Figure 6, and the May 1968 trails.

Figure 9. Estimates of the rate of dissipation of turbulent energy ε from the time of onset of turbulence for the releases of May 1968.

Figure 10. As for Figure 9, for the releases of October 1969. Note the presence of turbulent "sheets" alternating with laminar layers. Diurnally averaged dissipation rates for the month of October 1961 (Elford and Roper) and October 1969 (McAvaney) as measured by the radio meteor technique at Adelaide (35° S) are shown for comparison.

Figure 11. Isodensitrace of portion of the morning trail of October 16th, 50 seconds after release, showing the division into laminar and turbulent layers.

Figure 12. Theoretical morning temperature structure deduced from the profile of Figure 11.

Figure 13. An example of temperature structure in the lower stratosphere.

Figure 14. The turbulent vertical eddy diffusion coefficient (Kz) profiles deduced from the structure on the October 1969 releases, with the coefficient Δ deduced from simultaneous radio meteor observations at Adelaide (35° S), approximately 450 kilometers southeast of Woomera.

Figure 15. Vertical eddy diffusion coefficient profiles deduced from the rate of dissipation of turbulent energy profile at Wallops Island (38° N) - see Figure 6 - and the appropriate U.S. Standard Atmosphere Supplements, 1966, temperature profiles. Seasonal means for values deduced from radio meteor measurements at Adelaide (35° S) during 1961 and 1969 are shown for comparison.

Figure 16. The southern hemisphere mid latitude variation of vertical eddy diffusivity deduced from two years of radio meteor wind shear observations. Zimmerman's values result from a more vigorous analysis of the same 1961 data.

Figure 17. The seasonal variation of the southern hemisphere mid latitude diurnal tidal wind energy per unit mass. Equinoctial maxima are not a feature of all years.

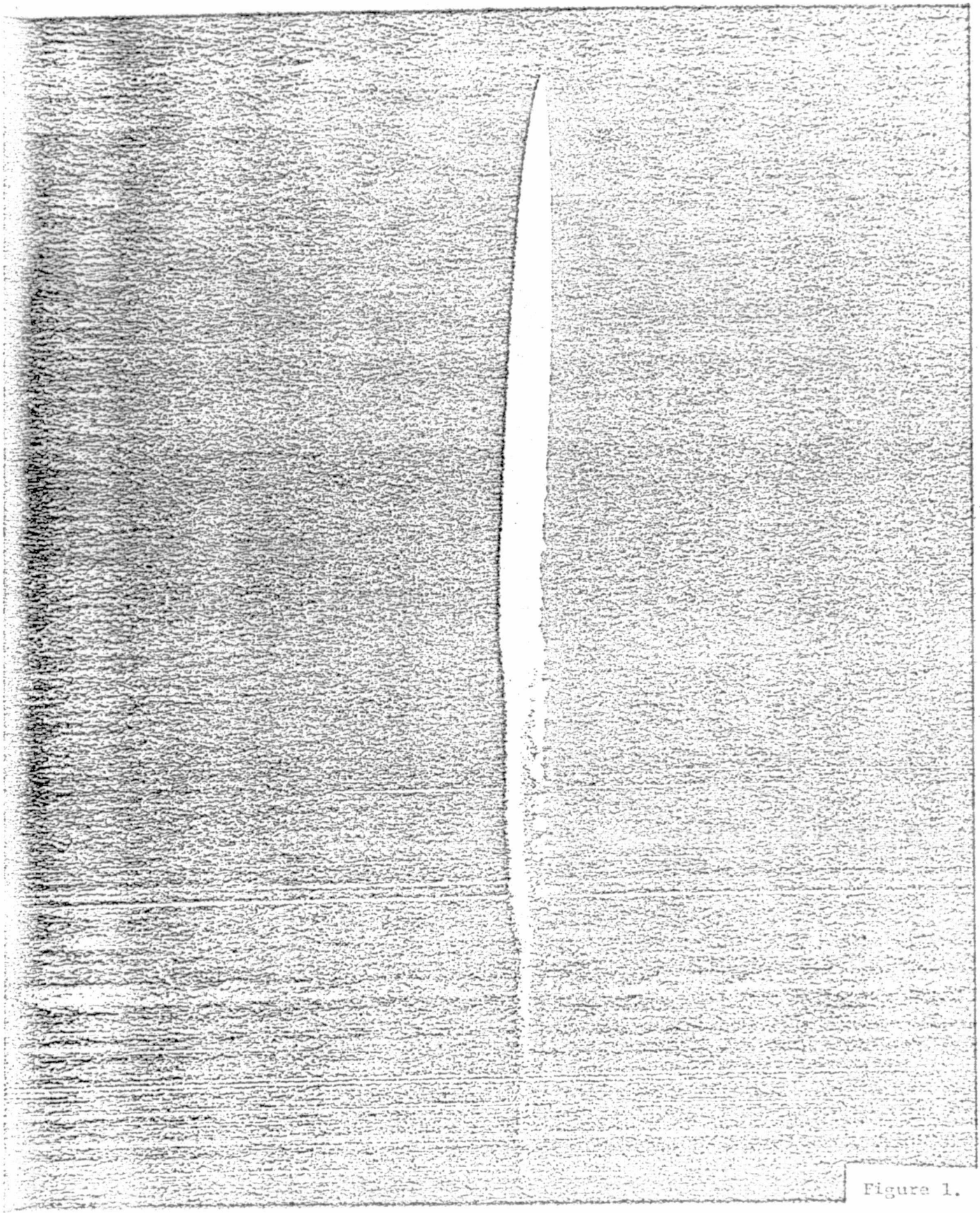

Figure 1.

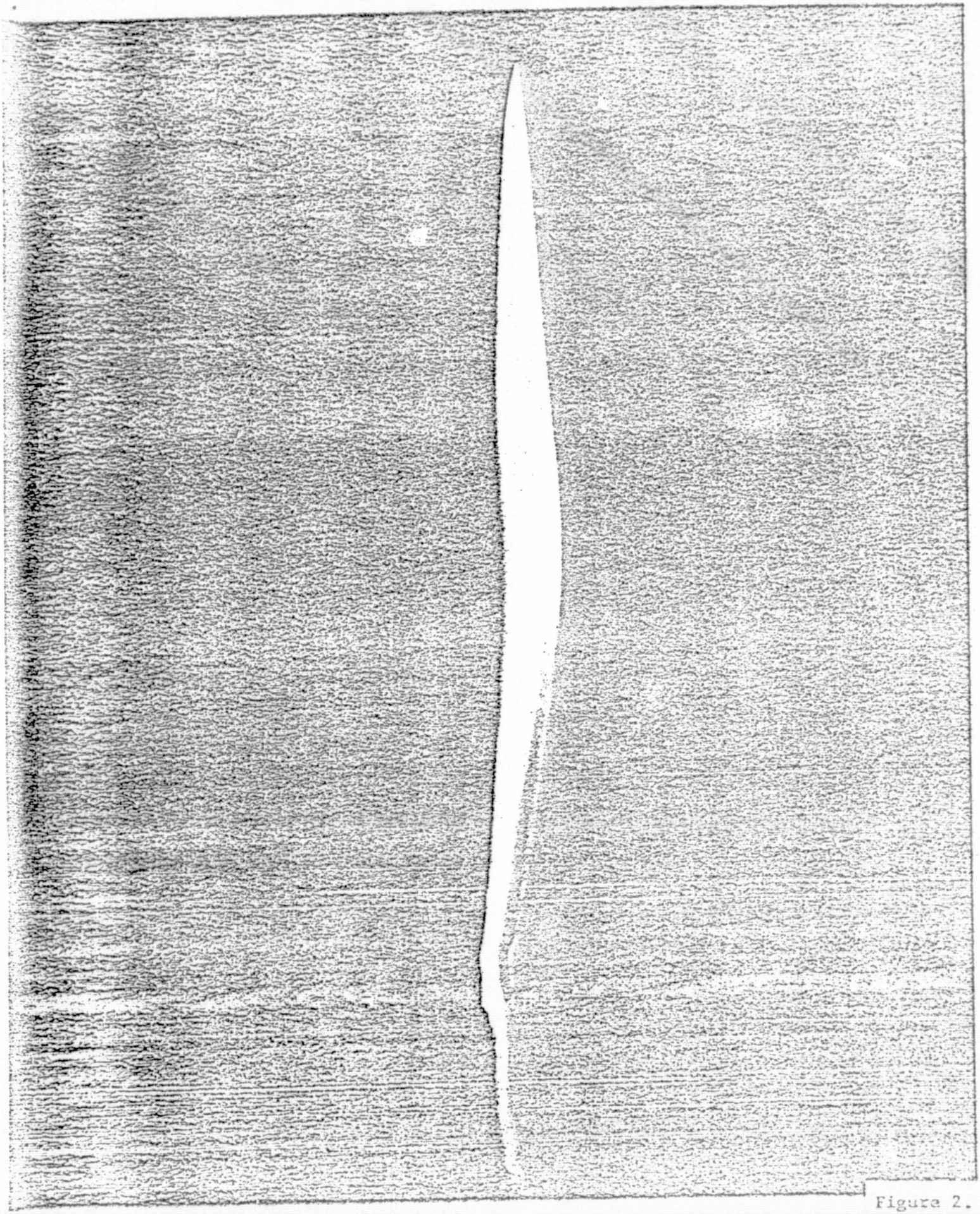

Figure 2.

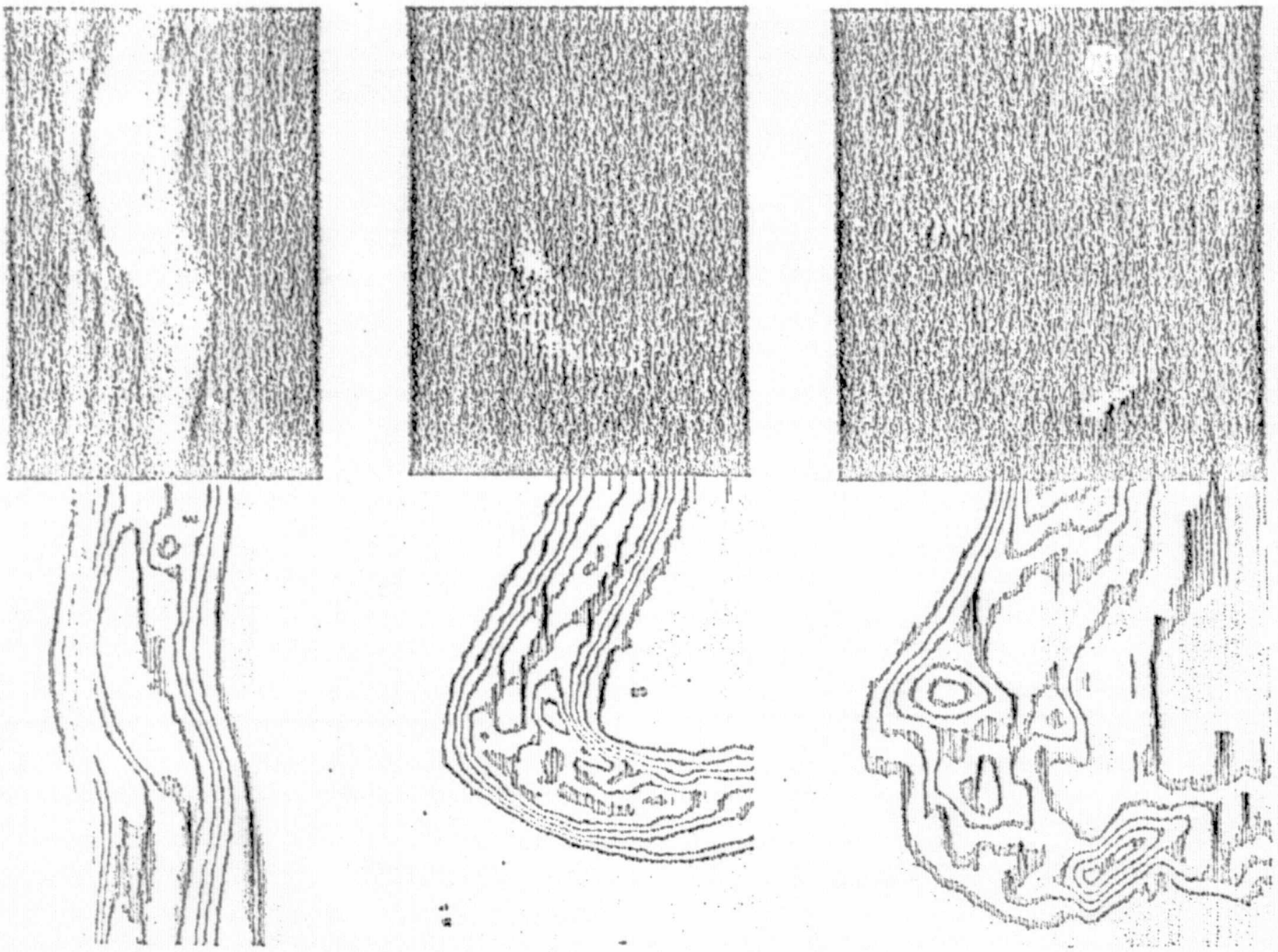

t = +5 sec. after release

+30 sec.

+50 sec.

The kink is at an altitude of 102·7 km.

1 km.

Note that the trail is laminar at +30 sec., and that the trail diameter at this time is greater than the scale of the eddies at +50 sec.

Figure 3.

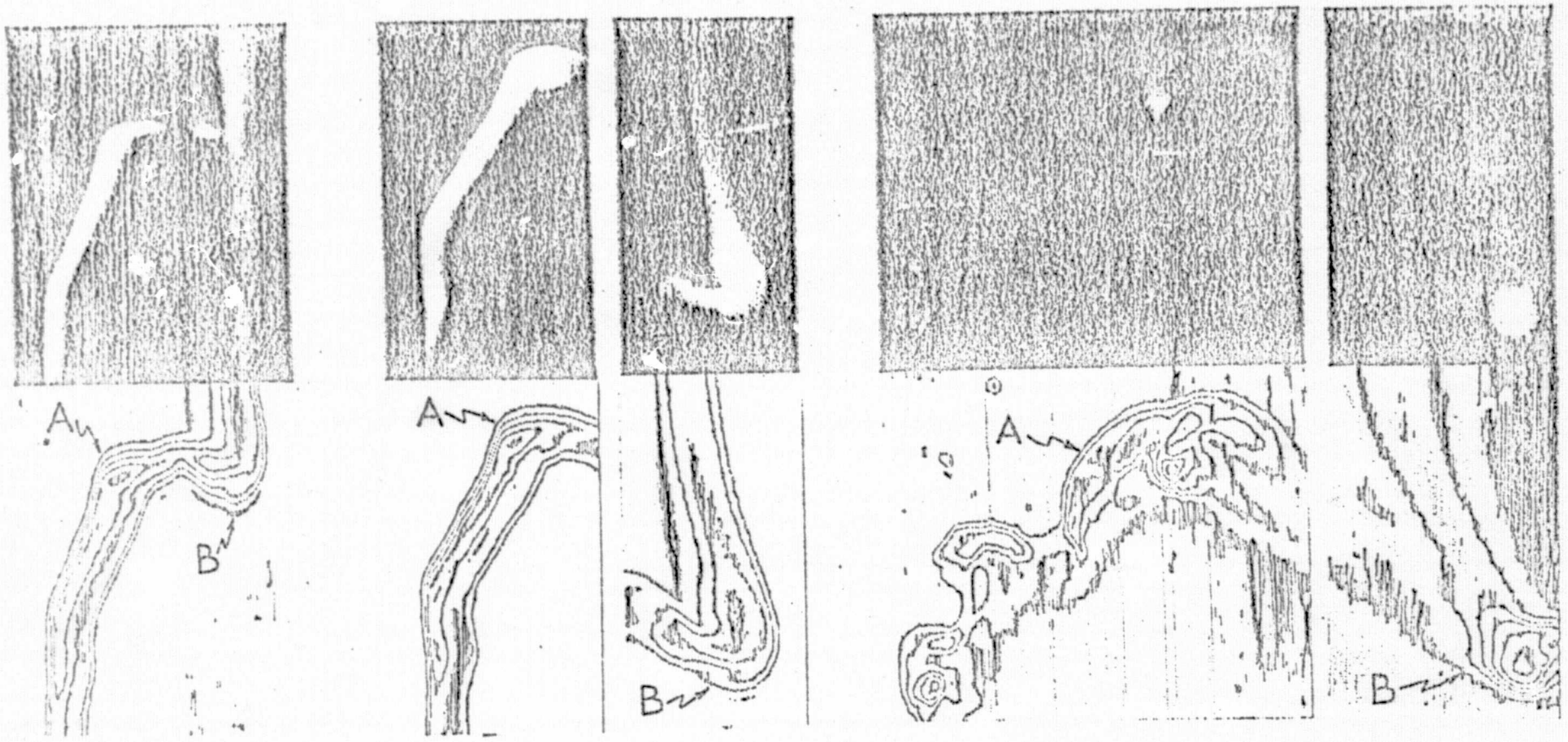

Points A and B are at 106 and 108 km altitude respectively.

Note the transition from laminar to turbulent structure at A between +23 and +61 sec. This has not occurred at B.

Figure 4.

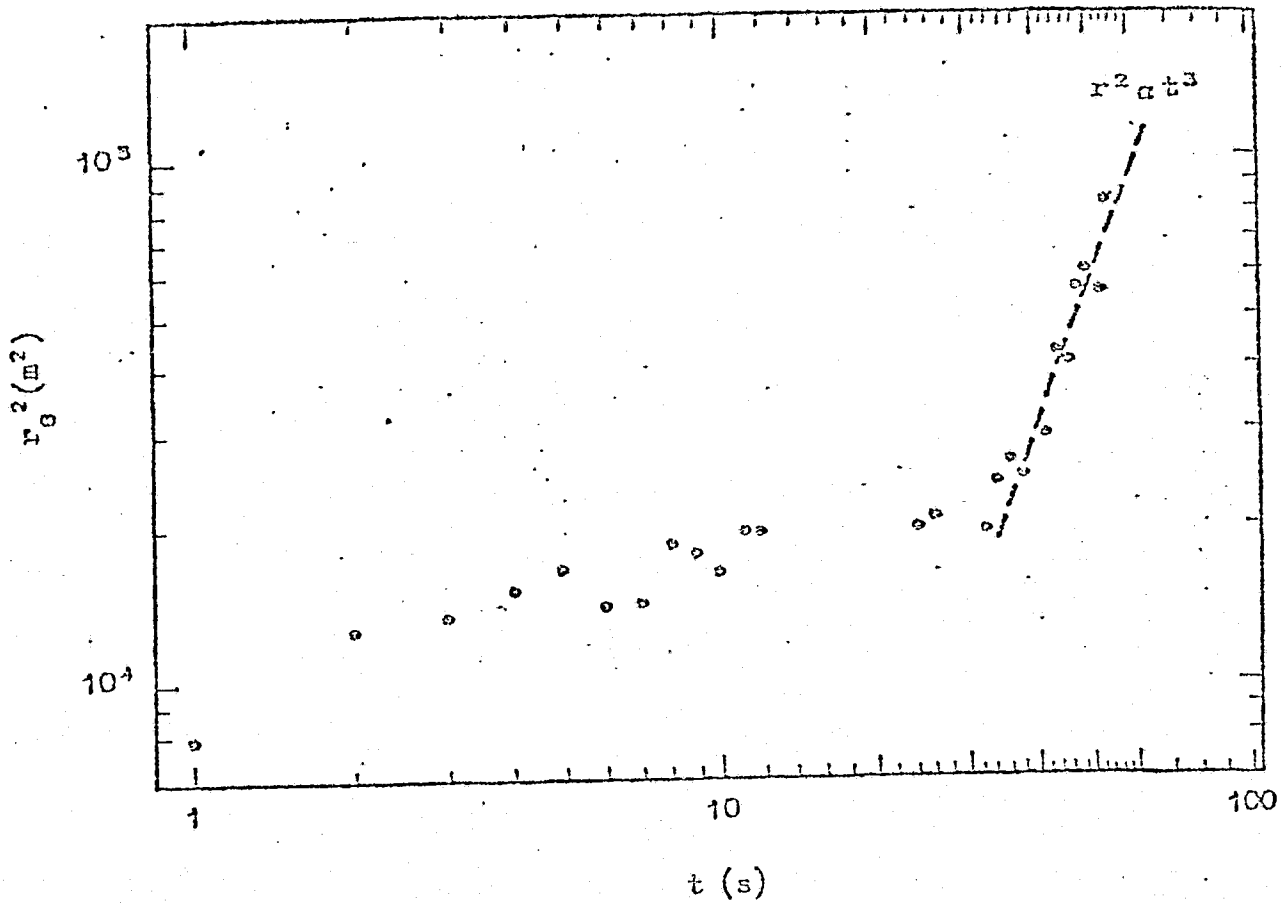

FIGURE 5

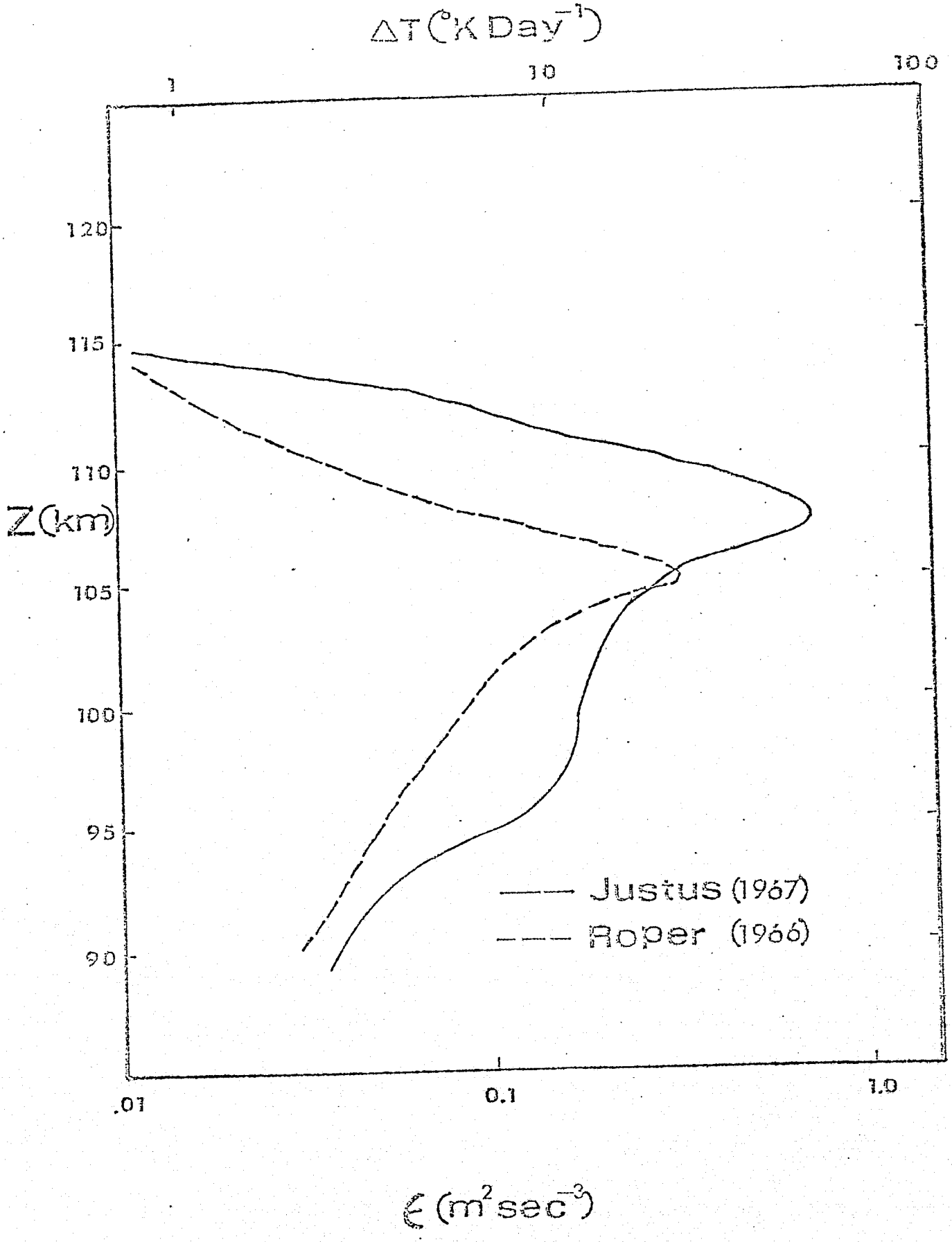
ΔT (°K Day⁻¹)
1
10
100
120
115
110
Z (km)
105
100
95
90
Justus (1967)
Roper (1966)
.01
0.1
1.0
ε (m² sec⁻³)

Figure 6.

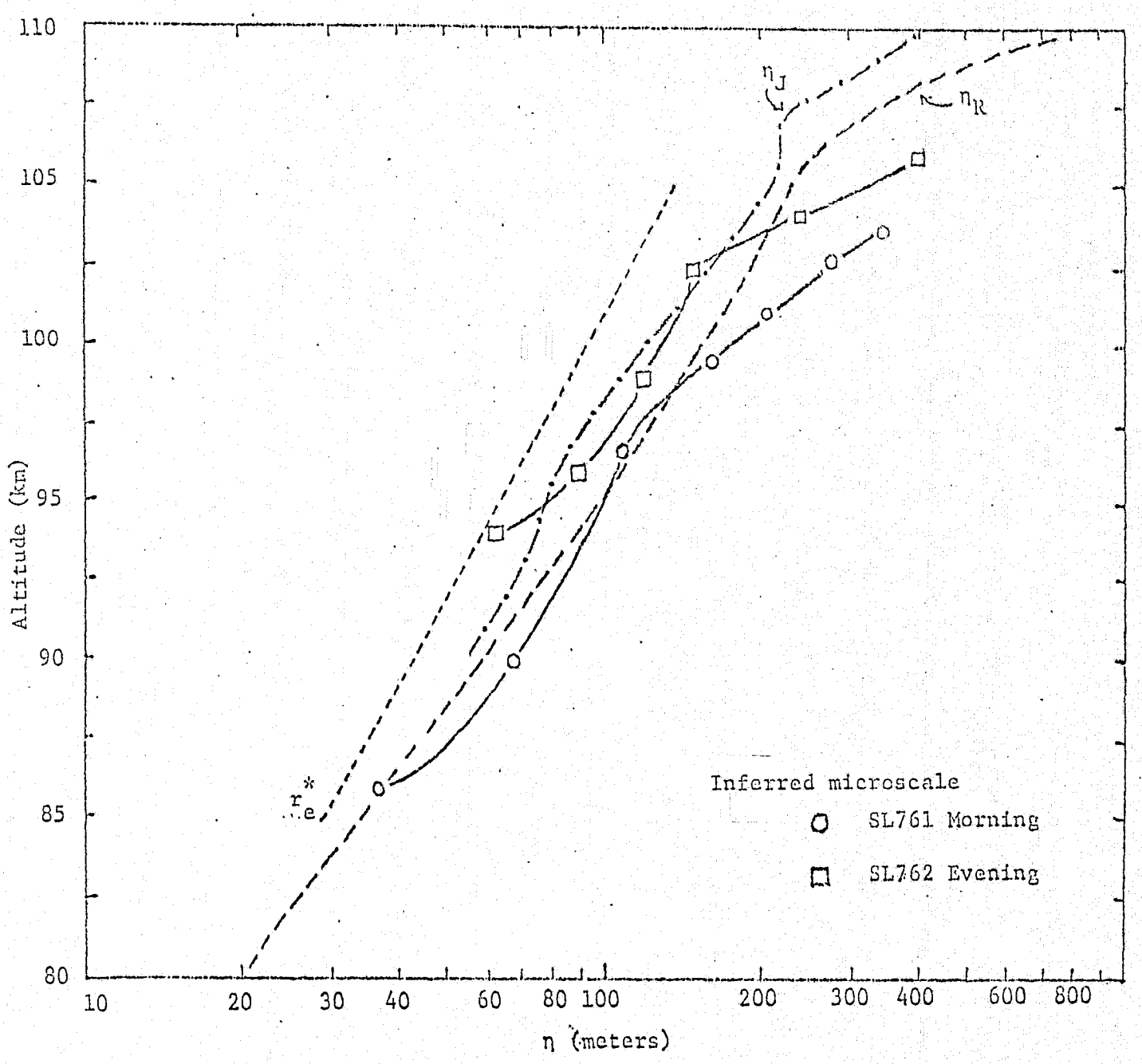
110
105
100
95
90
85
80
Altitude (km)
10
20
30
40
60
80
100
200
300
400
600
800
η (meters)
η_J
η_R
r_e^*
Inferred microscale
SL761 Morning
SL762 Evening

Figure 7.

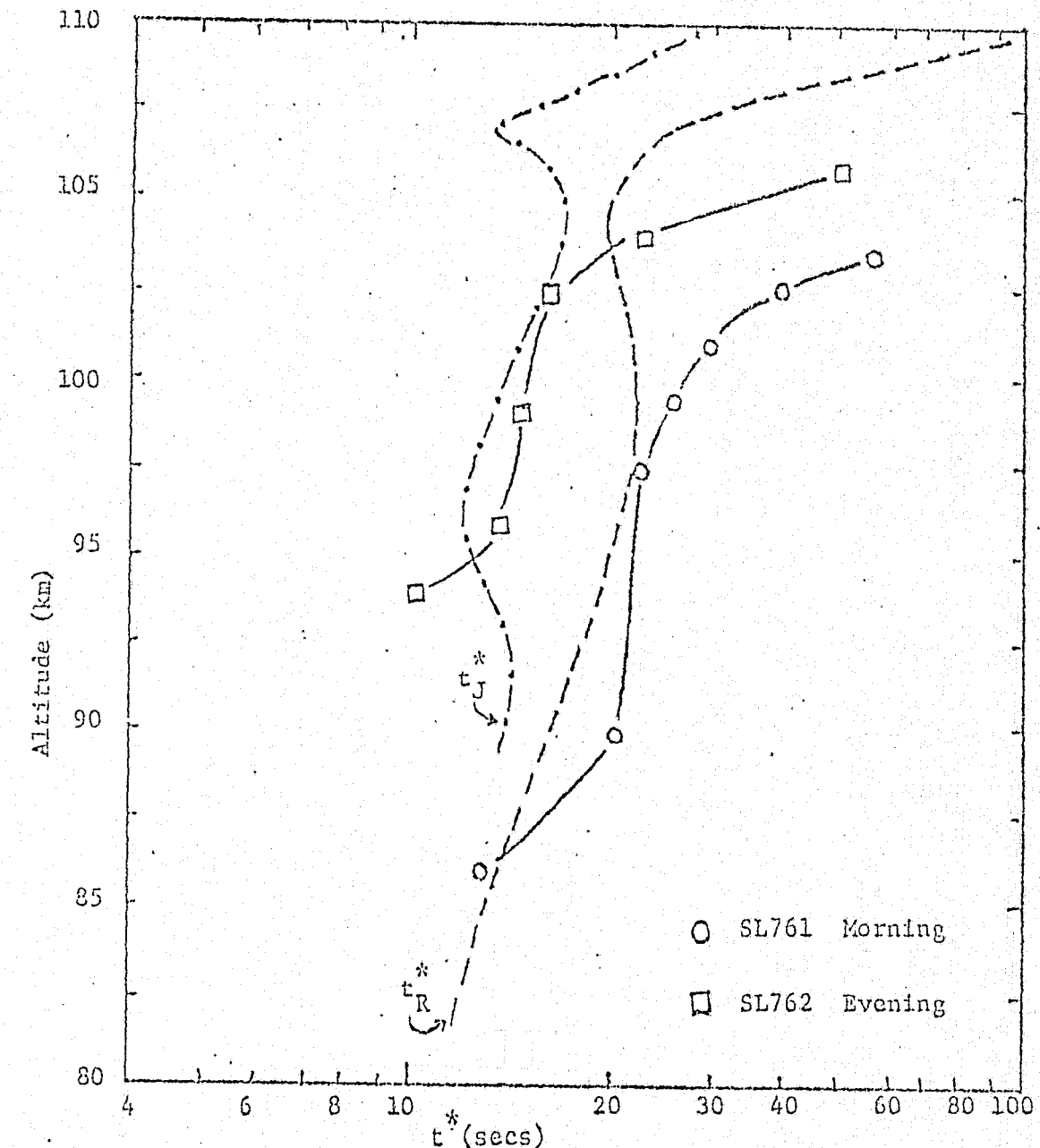
110
105
100
95
90
85
80
Altitude (km)
4
6
8
10
20
30
40
60
80
100
t* (secs)
t*J
t*R
SL761 Morning
SL762 Evening

Figure 8.

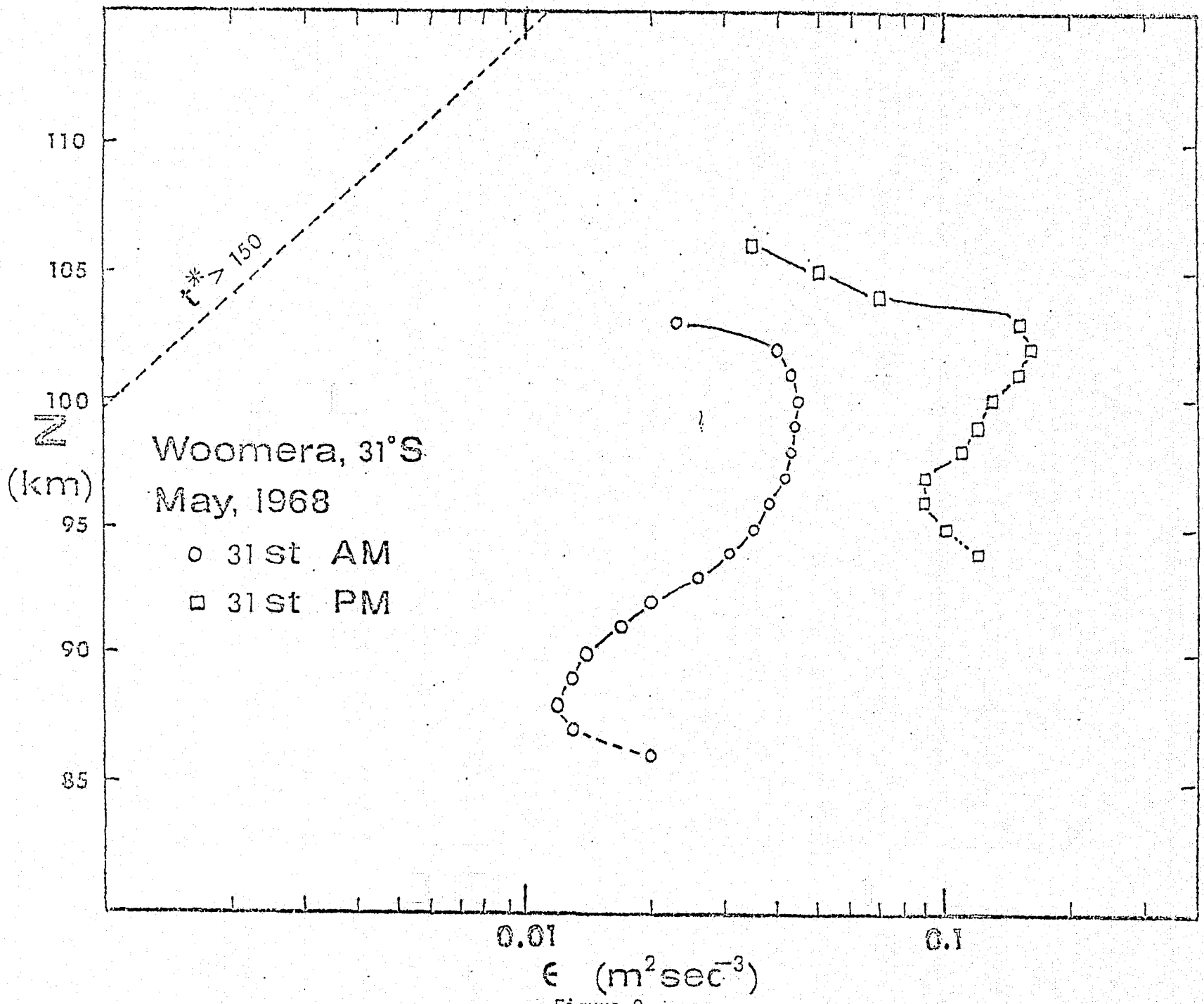
110
105
100
95
90
85
Z
(km)
$\ell^* > 150$
Woomera, 31°S
May, 1968
o 31st AM
□ 31st PM
0.01
0.1
ϵ ($m^2 sec^{-3}$)

Figure 9

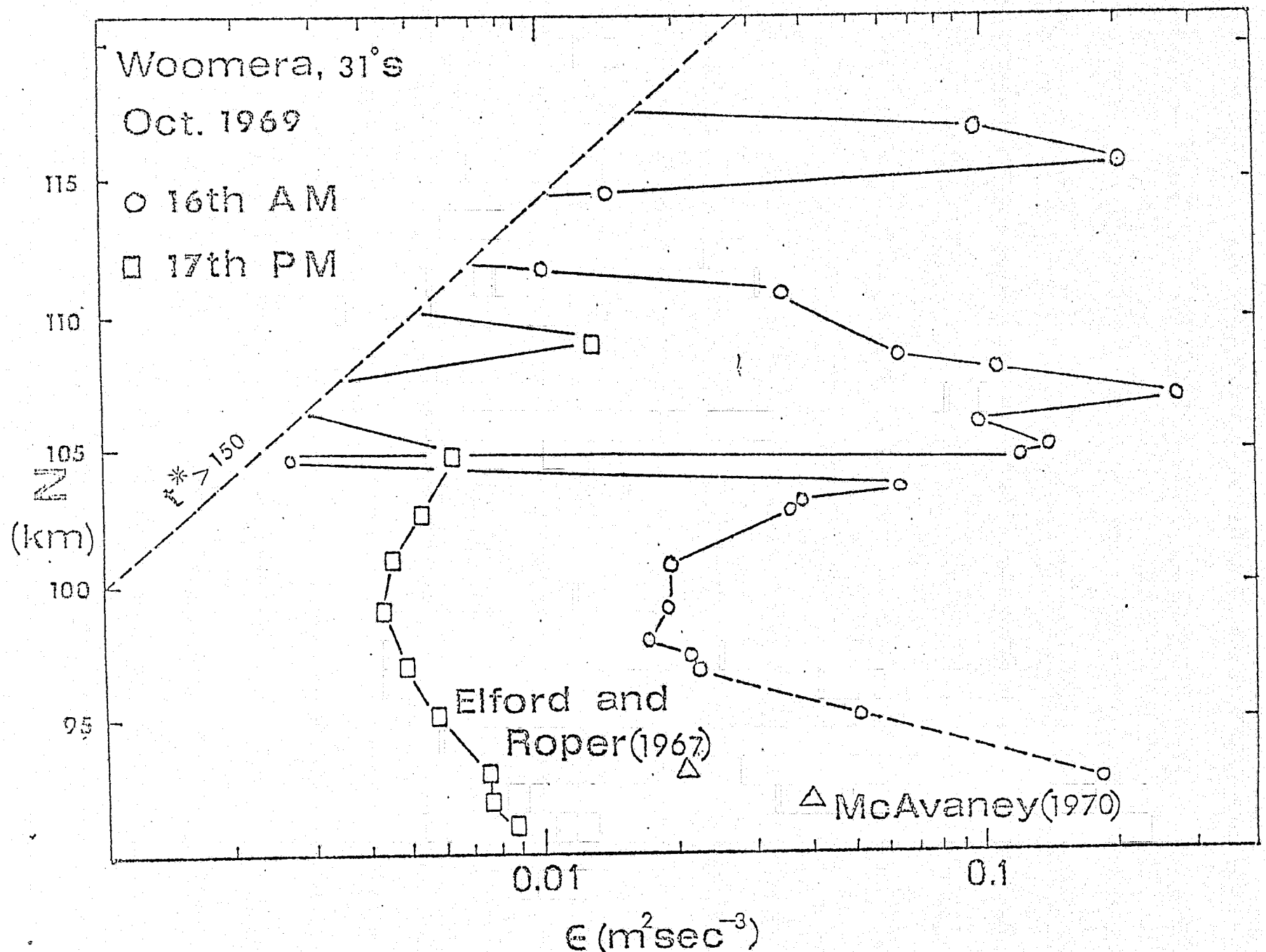
Woomera, 31°S
Oct. 1969
○ 16th AM
□ 17th PM
115
110
105
100
95
Z (km)
ε* = 150
Elford and Roper(1967)
McAvaney(1970)
0.01
0.1
ε (m²sec⁻³)

Figuee 10.

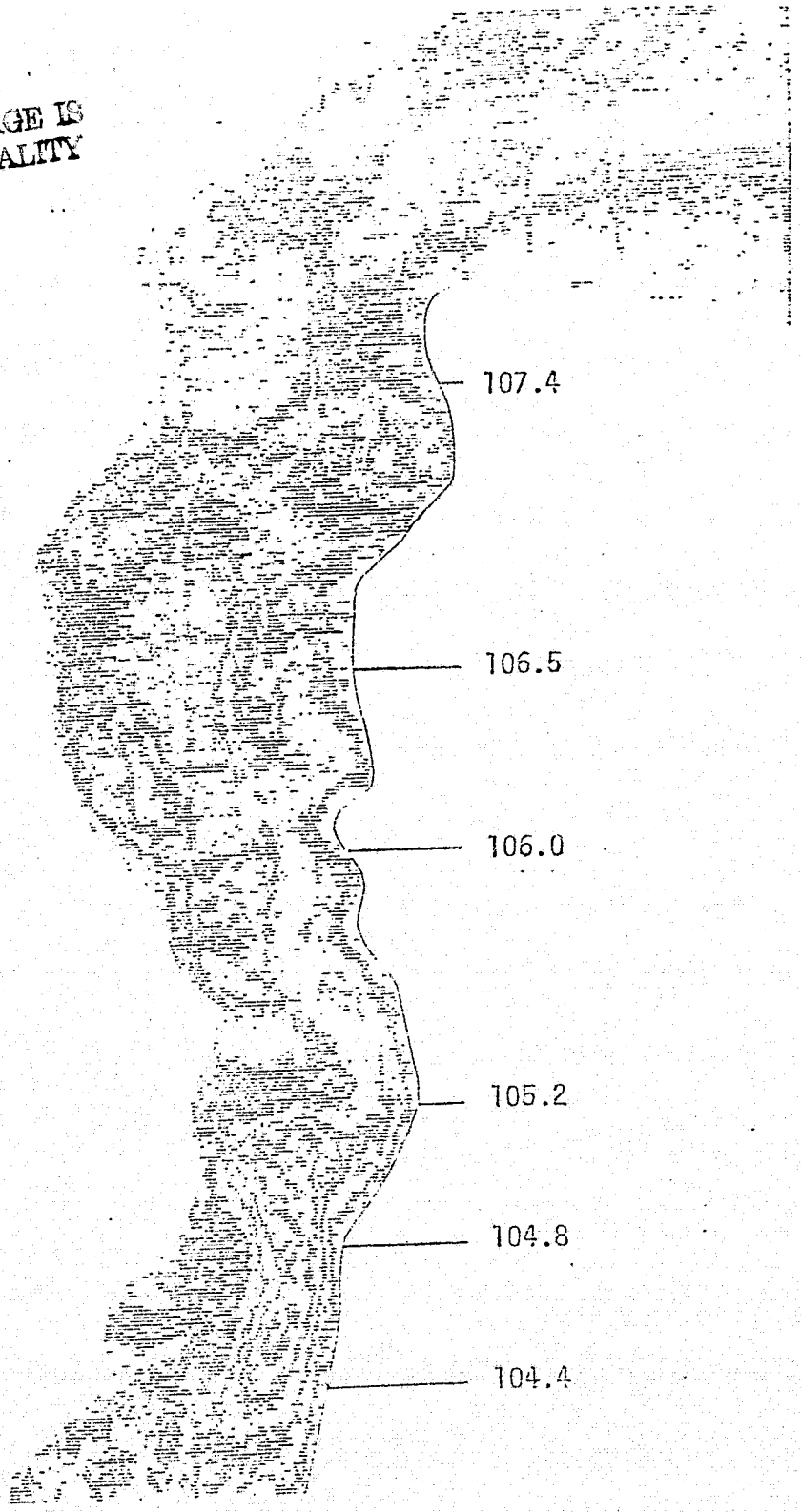

Figure 11.

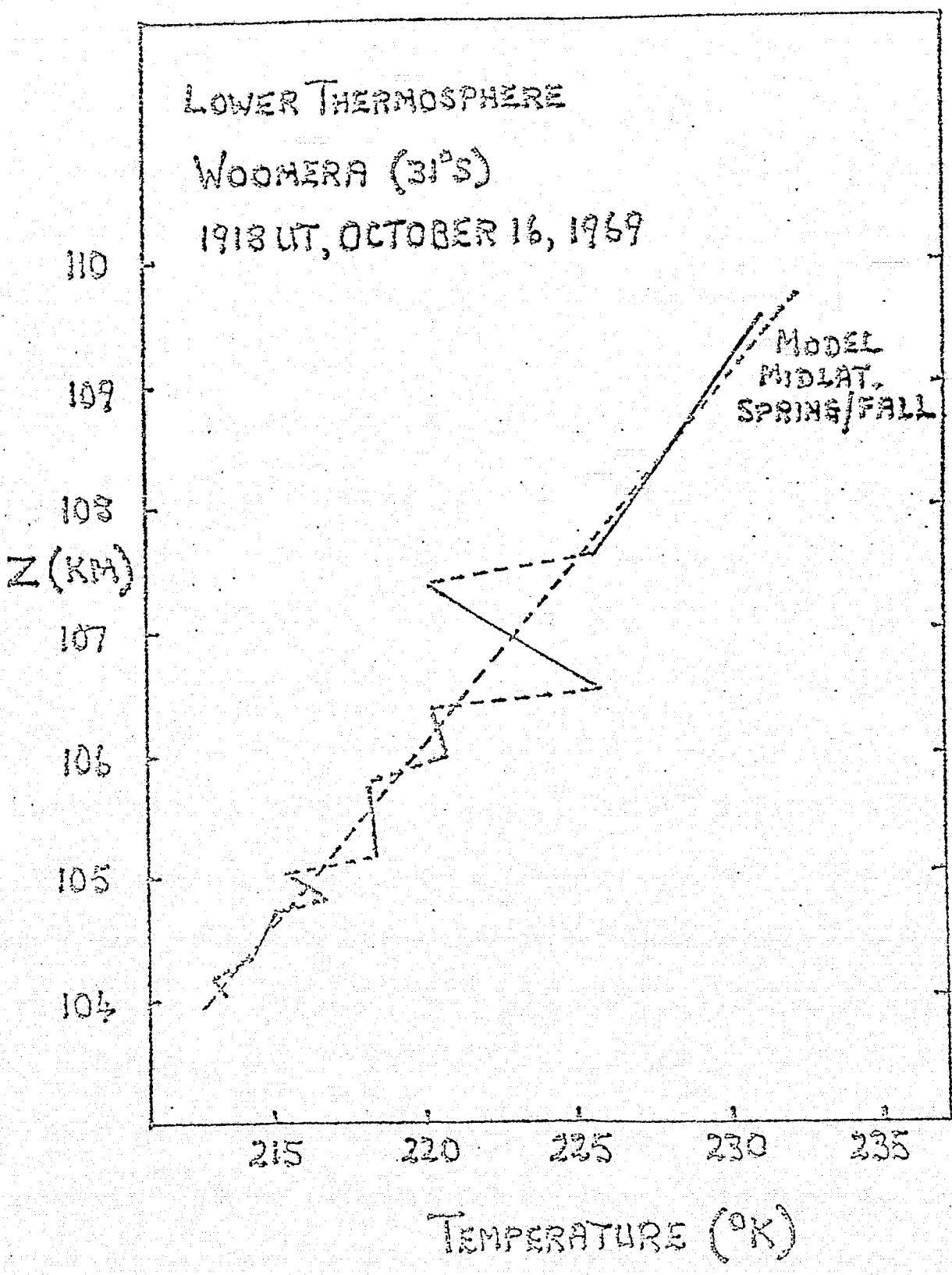

Figure : 12.

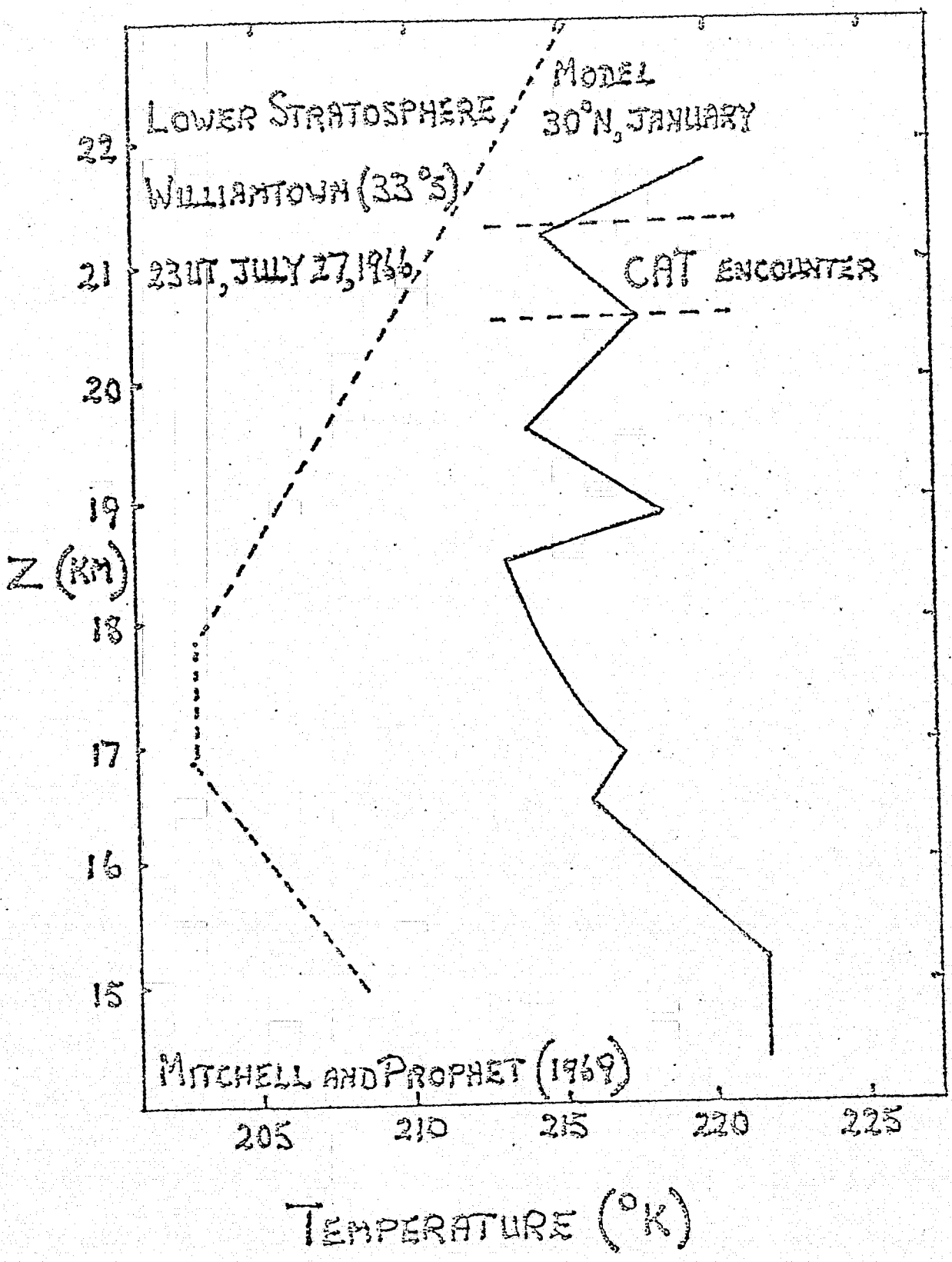
LOWER STRATOSPHERE,
WILLIAMTOWN (33°S),
23UT, JULY 27, 1966,
MODEL
30°N, JANUARY
CAT ENCOUNTER
MITCHELL AND PROPHET (1969)
Z (KM)
22
21
20
19
18
17
16
15
205
210
215
220
225
TEMPERATURE (°K)

Figure 13.

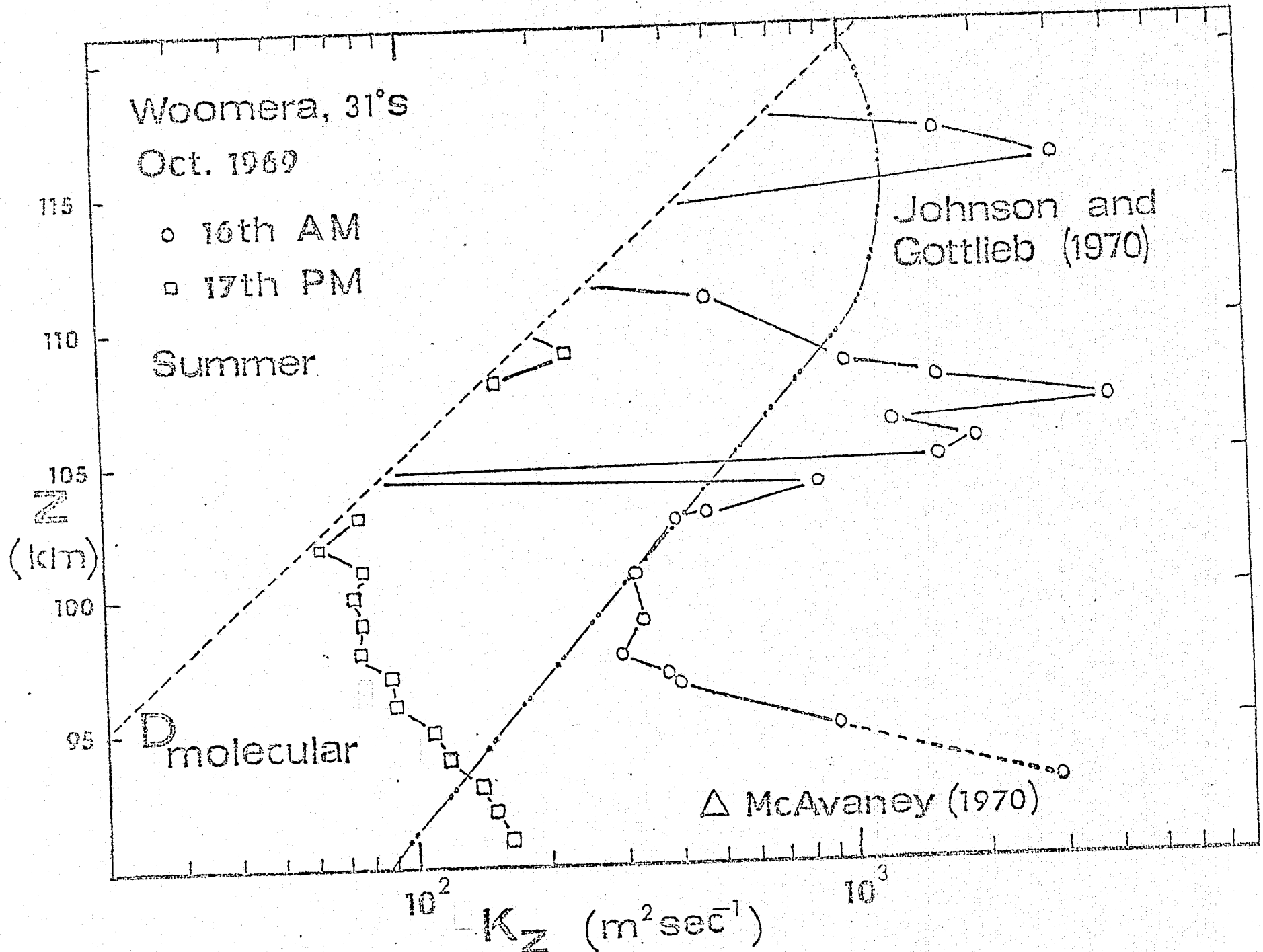
Woomera, 31°S
Oct. 1969
o 16th AM
□ 17th PM
Summer
Johnson and Gottlieb (1970)
Δ McAvaney (1970)
D molecular
115
110
105
100
95
Z (km)
10^2
10^3
K_Z ($m^2 sec^{-1}$)

Figure 14.

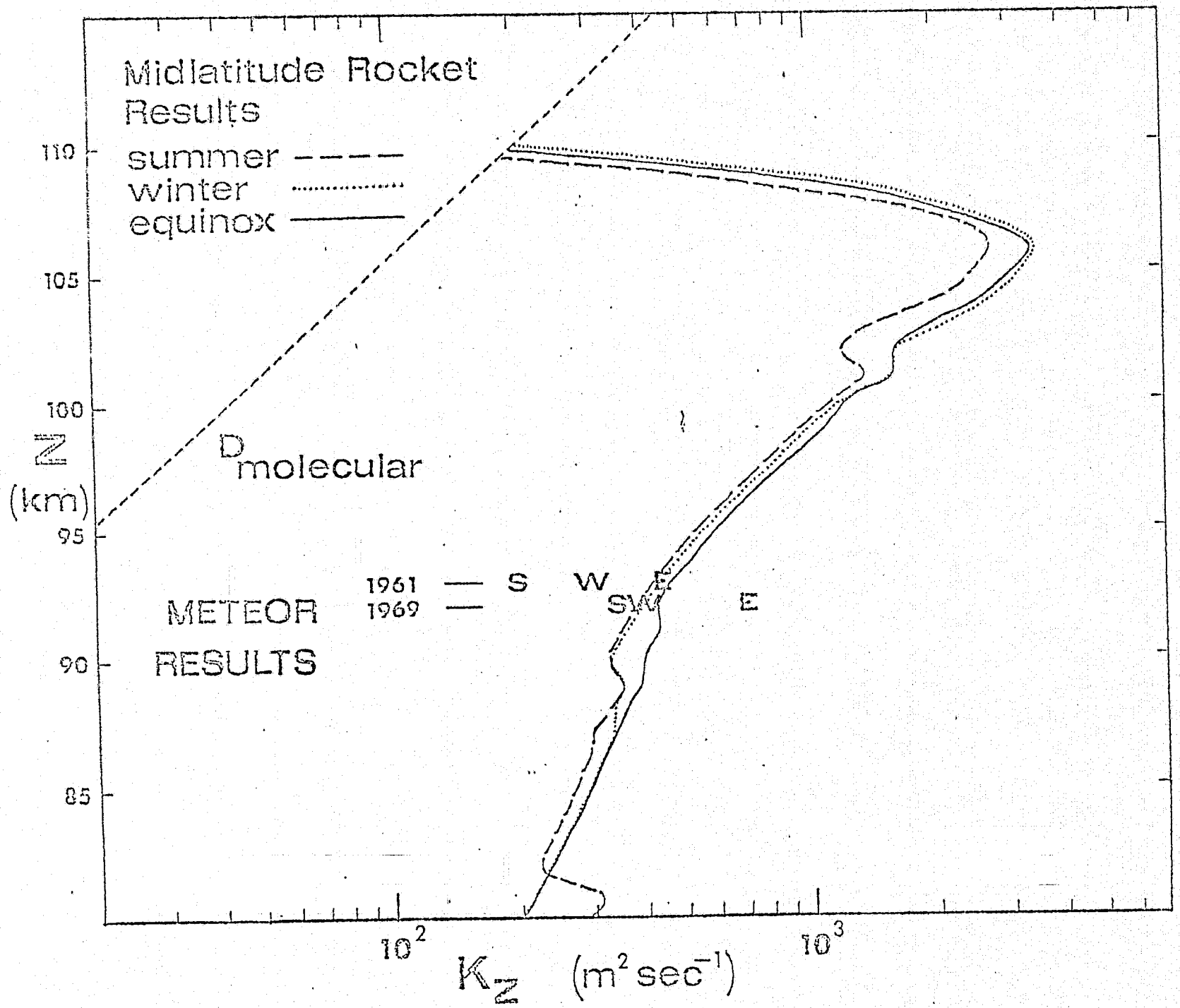
Midlatitude Rocket
Results
summer
winter
equinox
110
105
100
95
90
85
Z
(km)
D molecular
1961 — S W
1969 —
SW
E
METEOR
RESULTS
10^2
10^3
K_Z $(m^2 sec^{-1})$

Figuee 15.

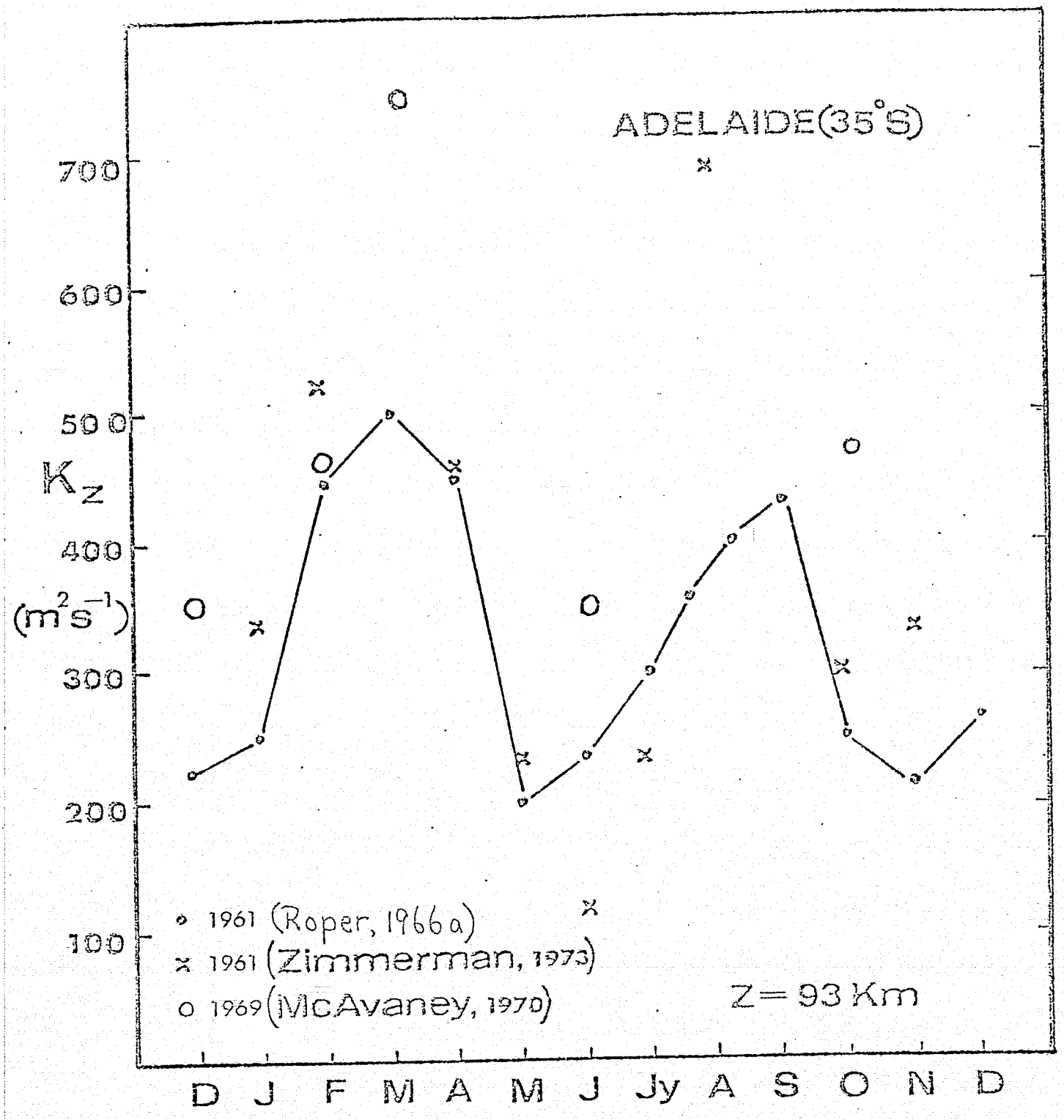
ADELAIDE(35°S)
700
600
500
400
300
200
100
K_z
(m^2s^{-1})
D J F M A M J Jy A S O N D
1961 (Roper, 1966a)
1961 (Zimmerman, 1973)
1969 (McAvaney, 1970)
Z = 93 Km

Figure 16.

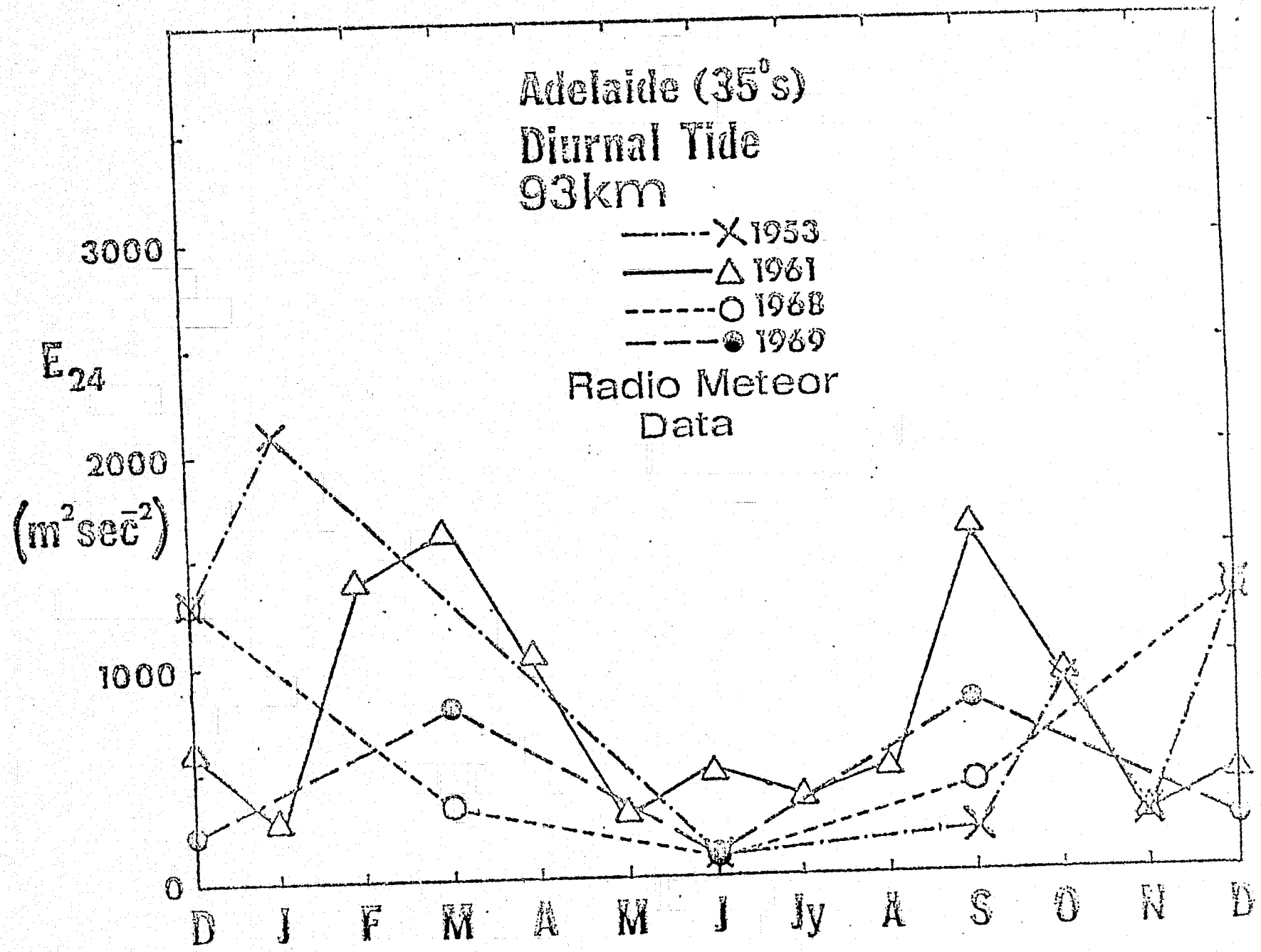
Adelaide (35°s)
Diurnal Tide
93km
1953
1961
1968
1969
Radio Meteor
Data
3000
2000
1000
0
E_{24}
$(m^2 sec^{-2})$
D
J
F
M
A
M
J
Jy
A
S
O
N
D

Figure 17.